A STUDY ON MHD FREE-CONVECTIVE FLOW IN MICRO-CHANNELS

BY

ABDURRAHMAN TUKUR AJIYA

DEPARTMENT OF MATHEMATICS,

FACULTY OF SCIENCE,

AHMADU BELLO UNIVERSITY, ZARIA

NIGERIA

JANUARY 2016

A STUDY ON MHD FREE-CONVECTIVE FLOW IN MICRO-CHANNELS

BY

ABDURRAHMAN TUKUR AJIYA
B. Sc (BUK, 2001)
P14SCMT8041

A THESIS SUBMITTED TO THE SCHOOL OF POSTGRADUATE STUDIES, AHMADU BELLO UNIVERSITY, ZARIA IN PARTIAL FULFILMENT OF THE REQUIREMENTS FOR THE AWARD OF MASTER OF SCIENCE DEGREE IN MATHEMATICS

DEPARTMENT OF MATHEMATICS, FACULTY OF SCIENCES,

AHMADU BELLO UNIVERSITY, ZARIA, NIGERIA

JANUARY 2016

DECLARATION

I, Abdurrahaman Tukur Ajiya declare that the work in this thesis titled "A STUDY ON MHD FREE-CONVECTIVE FLOW IN MICRO-CHANNELS" has been carried out by me in the Department of Mathematics under the supervision of Prof B. K. Jha and Dr A. O. Ajibade. The information derived from literature has been acknowledged in the text in accordance with what is required, and a list of references provided. No part of this thesis was previously presented for another degree or diploma at this or any other university/institution.

_____ _____

Signature Date

CERTIFICATION

This thesis entitled "A STUDY ON MHD FREE-CONVECTIVE FLOW IN MICRO-CHANNELS" by Abdurrahman Tukur Ajiya meets the regulation governing the award of the degree of Master of Science of the Ahmadu Bello University, Zaria and is approved for its contribution to knowledge and literary presentation.

Prof B. K. Jha	_____	_____
Chairman Supervisory Committee	Signature	Date
Dr A. O. Ajibade	_____	_____
Member Supervisory Committee	Signature	Date
Prof E. J. Garba	_____	_____
External Examiner	Signature	Date
Prof. B. Sani	_____	_____
Head of Department	Signature	Date
Prof K. Bala	_____	_____
Dean, School of Postgraduate Studies	Signature	Date

DEDICATION

This thesis is dedicated to Almighty ALLAH (S.W.T.) and my late parents Tukur Ajiya and Hannatu Hassan.

ACKNOWLEDGEMENT

Glory be to Almighty ALLAH (S. W. T.) for giving me the opportunity to write this thesis which is of course another step forward in my life. I sincerely wish to express my deep sense of gratitude to my major supervisor Prof. B. K. Jha and minor supervisor Dr A. O. Ajibade for putting me on track, and finding time to go through my work.

The knowledge acquired from my lecturers in the Department is worth commending and most prominent among them are: Late Dr Makarfi, Prof D. Singh, Prof. B. K. Jha, Prof. G. U. Garba, Prof. A. A. Tijjani, and Prof. J. Singh. The motivations I received from other lecturers of the Department such as Prof. B. Sani (Head of Department), Dr Dikko, Dr A. M. Ibrahim and Dr A. Mohammed were quite encouraging, and I highly appreciate that. I am also grateful to all other lecturers and staff of the Department.

My sincere gratitude goes to my M.Sc. colleagues Shehu A. Muhammad, Kabir M. Musa, Aina Babatunde and the entire staff of ABU/SBRS Funtua for their words of courage and motivation.

Lastly, my in-depth gratitude goes to my family and the entire family of late Tukur Ajiya for their support, prayers and guidance, and also to Ahmadu Bello University, Zaria and School of Basic and Remedial Studies, Funtua, for giving me the privilege to undertake this program.

ABSTRACT

This work analyses the steady natural convection flow of viscous, incompressible, electrically conducting fluid in a vertical parallel plate micro-channels with combined effects of transverse magnetic field and suction/injection in the presence of velocity slip and temperature jump at the micro-channel surfaces. The fully developed solutions of the velocity, temperature, volume flow rate, skin-friction and rate of heat transfer which is expressed as a Nusselt number are derived analytically. The solution obtained for the velocity has been used to compute the skin friction, while the temperature has been used to compute the Nusselt number. The effect of the various flow parameters such as suction/injection parameter, Hartmann number, rarefaction parameter, and fluid-wall interaction parameter are discussed with the aid of line graphs. During the course of numerical computations, results show that as suction/injection, rarefaction and fluid-wall interaction increase, the volume flow rate increases while it decreases with increase in Hartmann number. The implication of this on the flow is that the gas velocity near the wall will decrease.

TABLE OF CONTENTS

Cover Page……i
Fly Leaf……ii
Title Page……iii
Declaration……iv
Certification……v
Dedication……vi
Acknowledgement……vii
Abstract……viii
Table of Contents……ix
List of Figures……x
List of Appendices……xi
Notations……xiii
Basic Definitions……xv
Dimensionless Quantities……,xvi

CHAPTER ONE

GENERAL INTRODUCTION

1.0 Introduction i
1.1 Aim and Objectives of Study 2
1.2 Research Methodology 2
1.3 Organization of the Thesis 3

CHAPTER TWO

LITERATURE REVIEW

2.0 Introduction 4
2.1 MHD Natural Convection Flow in Vertical Parallel Plate Micro-channels 6
2.2 Suction/Injection on MHD Natural Convection in Vertical Parallel Plate Micro-channels 8

CHAPTER THREE

MATHEMATICAL ANALYSIS AND METHOD SOLUTIONS

3.0 Introduction xi
3.1 MHD Natural Convection Flow in Vertical Parallel Plate Micro-channels 11
3.1.1 Mathematical Analysis 11
3.2 Suction/Injection on MHD Natural Convection in Vertical Parallel Plate Micro-channels……13
3.2.1 Mathematical Analysis 11

3.3 Non Dimensionalisation 15
3.4 Solution to Problems 17
3.4.1 Solution for MHD Natural Convection in Vertical Parallel Plate Micro-channels.17
3.4.2 Solution to Suction/Injection on MHD Natural Convection in Vertical Parallel Plate Micro-channels 18

CHAPTER FOUR

RESULTS AND DISCUSSIONS

4.0 Introduction 20
4.1 Results for MHD Natural Convection Flow in Vertical Parallel Plates Micro-channels 20
4.2 Results for Suction/Injection on MHD Natural Convection in Vertical Parallel Plate Micro-channels 27

CHAPTER FIVE

SUMMARY, CONCLUSIONS AND RECOMMENDATIONS

5.0 Introduction 37
5.1 Summary 37
5.2 Conclusion 38
5.3 Recommendations 39
REFERENCES……..……...40
APPENDIX I 44
APPENDIX II 45
APPENDIX III 46

LIST OF FIGURES

Figure 3.1: Flow configuration and coordinate system of the first problem……..……12

Figure 3.2: Flow configuration and coordinate system of the second problem…….14

Figure 4.1.1: Velocity profile for various values of $\beta_v Kn$ (*ln = 1.667, M = 2.0*)……..23

Figure 4.1.2: Velocity profile for various values of *ln* ($\beta_v Kn$ *= 0.05, M = 2*……..23

Figure 4.1.3: Velocity profile for various values of *M* ($\beta_v Kn$ *= 0.05, ln = 1.667*)……24

Figure 4.1.4: Relationship of Volume flow rate to $\beta_v Kn$ for various values of *ln*……24

Figure 4.1.5: Relationship of Volume flow rate to $\beta_v Kn$ for various values of *M*……25

Figure 4.1.6: Relationship of skin friction to various values of *ln* (*Y = 0*)……25

Figure 4.1.7: Relationship of skin friction to various values of *ln* (*Y = 1*)……26

Figure 4.1.8: Relationship of skin friction to various values of *M* (*Y = 0*)……26

Figure 4.1.9: Relationship of skin friction to various values of *M* (*Y = 1*)……27

Figure 4.2.1: Velocity profile for various values of $\beta_v Kn$ (*ln = 1.667, S = 0.5, M = 2.0, Pr = 0.71*)...30

Figure 4.2.2: Velocity profile for various values of *ln* ($\beta_v Kn$ *= 0.05, S = 0.5, M = 2.0, Pr = 0.71*)….31

Figure 4.2.3: Velocity profile for various values of *M* ($\beta_v Kn$ *= 0.05, S = 0.5, ln = 1.667, Pr = 0.71*).31

Figure 4.2.4: Velocity profile for various values of *S* ($\beta_v Kn$ *= 0.05, M = 2.0, ln = 1.667, Pr=0.71*)...32

Figure 4.2.5: Relationship of Volume flow rate to βvKn for various values of *ln*……32

Figure 4.2.6: Relationship of Volume flow rate to $\beta_v Kn$ for various values of *M*……33

Figure 4.2.7: Variation of skin friction to various values of *ln* (*S = 0.5, M = 2.0* (*Y = 0*))……..xii33

Figure 4.2.8: Variation of skin friction to various values of *ln* (*S = 0.5, M = 2.0* (*Y = 1*))……...34

Figure 4.2.9: Variation of skin friction to various values of *M* (*S = 0.5, ln = 1.667* (*Y = 0*))……34

Figure 4.2.10 Variation of skin friction to various values of *M* (*S = 0.5, ln = 1.667* (*Y = 1*))……..35

Figure 4.2.11: Variation of skin friction to various values of *S* (*M = 2.0, ln = 1.667* (*Y = 0*))……**Error! Bookmark not defined.**35

Figure 4.2.12: Variation of skin friction to various values of *S* (*M = 2.0, ln = 1.667* (*Y = 1*))…….36

LIST OF APPENDICES

Appendix I: - List of constants used in Problem 3.1

Appendix II: - List of constants used in Problem 3.2

Appendix III: - Computer program for the role of magnetohydrodynamic (MHD) natural convection flow in vertical parallel plate micro-channels

Appendix IV: - Computer program for the combined role of transverse magnetic field suction/injection on the magnetohydrodynamic (MHD) natural convection flow in vertical micro-channels

NOTATIONS

NOMENCLATURE

b channel width

B_0 strength of applied magnetic field

C_p, C_v Specific heats at constant pressure and constant volume, respectively

f_t, f_v thermal and tangential momentum accommodation coefficients, respectively

g gravitational acceleration

In fluid- wall interaction parameter, β_t/β_v

Kn Knudsen number, λ/b

m volume flow rate

Q dimensionless volume flow rate

M Hartmann number

Nu dimensionless heat transfer rate (Nusselt number)

Pr Prandtl number

T temperature of fluid

T_0 reference temperature

V_0 constant of suction and injection

u velocity components in x direction

U dimensionless velocity

GREEK LETTERS

α thermal diffusivity

β thermal expansion coefficient

β_t, β_v dimensionless variables

γ_s ratio of specific heats (C_p/C_v)

μ dynamic viscosity

θ dimensionless temperature

ξ wall-ambient temperature difference ratio

ρ density

ν fluid kinematic viscosity

σ electrical conductivity of the fluid

SUBSCRIPTS

1 hotter wall values

2 cooler wall values

BASIC DEFINITIONS

1. **Free Convection:** It is a mechanism or type of heat transport, in which the fluid motion is not generated by any external source (like pump, fan, suction device etc), but only by density differences in the fluid occurring due to temperature gradient or concentration gradients or both.

2. **Suction/Injection:** The simplest active flow control system is surface suction/injection as they significantly affect the flow field. Controlling fluid flow within vertical channel with suction and injection is an interesting exercise as both activities are carried out simultaneously on opposite channel plates. The influence of suction on rate of heat transfer and skin friction is opposite to the influence of injection (Ajibade, 2009).

3. **Porous:** It is the permission of the movements of liquid or gases, or microscopic particles through a solid surface by way of pores.

4. Skin Friction: It is the amount of friction occurring between the fluid and the surface of the plates which tends to slow the movement of the fluid and is given by: $\tau = \left.\frac{dU}{dy}\right|_{y=0,\, y=H}$

5. Nusselt Number (Nu): This is the rate of heat transfer at the wall-fluid boundary and it is defined by: $Nu = \left.\frac{d\theta}{dy}\right|_{y=0,\, y=H}$

6. Boussinesq Approximation: The natural convectional flow is governed by complex couple of partial differential equations. Boussinesq Approximation is employed to simplify the computation. It is assumed that the flow is considered under little variation of temperature and density.

DIMENSIONLESS QUANTITIES

There are some dimensionless quantities that are usually used in fluid mechanics in order to determine relationship between parameters and to generalize results so as to predict performance for different systems. Some of these dimensionless quantities are used in this thesis. They include:

1. **Prandtl number (Pr):** This is the ratio of momentum to thermal diffusivities and is a function only of fluid property. Pr is typically less than 1 for gases and greater than 1 for liquids. Prandtl number can be expressed mathematically as: $\Pr = \frac{\nu}{\alpha}$, where α and ν are defined in the nomenclature herein.

2. **Knudsen Number (Kn):** It is a dimensionless number defined as the ratio of the molecular mean free path length to a representative physical length scale. This length scale could be, for example, the radius of the body in a fluid. Knudsen number is expressed mathematically as: $Kn = \frac{\lambda}{b}$, where λ and b are defined in nomenclature herein.

3. **Hartmann Number (M):** It is the ratio of electromagnetic force to the viscous force first introduced by Hartmann. It is mathematically expressed as: $M = \beta_0 b \sqrt{\frac{\sigma}{\rho\nu}}$, where $\beta_{0,}\ b, \sigma, \rho$ and ν are defined in the nomenclature herein.

CHAPTER ONE

GENERAL INTRODUCTION

1.0 Introduction

Microflow has been given great importance in recent research activities due to its new application in microfluidic system devices, such as biomedical sample injection, biochemical cell reaction, microelectric ship cooling, etc. A fundamental understanding of the flow and thermal fields as well as the corresponding characteristics at microscale, which may deviate from those at macroscale, is required for the technological demands.

Gaseous flow in microscale devices have been in the vanguard of research activities and have received great deal of attentions in recent years, due to the rapid growth of application in micrototal analysis systems and micro electromechanical systems (MEMS). These applications have raised the interest in understanding the physical aspects of fluid flow and convective heat transfer in both forced and natural forms through micron sized channels, known as micro-channels.

A magnetohydrodynamic (MHD) flow, which is the simplest plasma model, has been the subject of a great number of empirical and theoretical investigations in many industrial fields. MHD flows associating with heat transfer have received considerable attention due to the fact that their applications reside in many industrial fields such as electric propulsion for space exploration, crystal growth in liquids, cooling of nuclear reactors, electronic packages, microelectronic devices, etc.

The most common type of body force, which acts on fluid, is attributed to gravity so that the body force vector can be deduced from the gravitational acceleration. On the other hand, when an electrically conducting fluid is subjected to a magnetic field, the fluid motion

induces an electric current such that the fluid velocity is reduced on account of interaction between the electric current and the fluid motion. Therefore, in case of free convection of an electrically conducting fluid in the presence of a magnetic field, there should be two body forces, i.e., a buoyancy force and a Lorentz force. They interact with each other, and in turn influence the transport phenomena of heat and mass.

Among various studies of MHD free flows, few studies have been accomplished for the confined enclosures. Seki *et al*. (1979) studied the laminar natural convection of mercury subjected to a magnetic field parallel to gravity in a rectangular enclosure. Numerical results were obtained and compared to their experiment in the consideration of a partially heated vertical wall by uniform heat generator. Rudraiah et al. (1995) performed a numerical simulation about natural convection in a two-dimensional cavity filled with an electrically conducting fluid in the presence of a magnetic field aligned to gravity. They selected the Grashof and Hartmann numbers as controlling parameters to examine the effect of a magnetic field on free convection and associated heat transfer.

Some research works were carried out on natural convection in a vertical micro-channel. Example of which are Yu and Ameel (2001), Cheng and Weng (2005) and Jha *et al*. (2013). Details are given in literature review.

1.1 Aim and Objectives of Study

The aim of this work is to study a fully developed natural convection flow of viscous, incompressible, electrically conducting fluid in a micro-channels formed by two vertical parallel plates under the effects of transverse magnetic field and suction/injection and this is achieved through the following objectives:

i. investigate the influence of external applied transverse magnetic field on steady natural convection flow of conducting fluid in vertical parallel plate micro-channels, and

ii. investigate the combined influence of external applied transverse magnetic field and suction/injection on steady natural convection flow of conducting fluid in vertical parallel plate micro-channels

1.2 Research Methodology

The methodology adapted in this thesis in order to achieve the set objectives is by dividing the work into five-stages. In the first stage, we reviewed some existing literature and extended them to include new parameters. Second stage is concerned with solving the mathematical model to obtain analytical solutions. In the third stage, the numerical values of the analytical solutions of the developed equations are obtained by computer package (MATLAB). The fourth stage is the graphical representation of the problems, and the last stage is the interpretation of the graphs so as to discuss the influence of each of the governing parameters and conclusions.

1.3 Organization of the Thesis

A study on MHD free-convective flow in vertical parallel plates micro-channels is a five-chapter thesis in order to achieve the objectives of the work. Chapter one introduces the objectives of the study and the method adopted to achieve the set objectives. Chapter two basically reviews existing literature. Chapter three gives the mathematical analysis and solutions of the governing equations with their non-dimensionalisation. While chapters four and five gives the discussion of the results/graphs, summary, concluding remarks and recommendations.

CHAPTER TWO

LITERATURE REVIEW

2.0 Introduction

There has been considerable interest in studying flows of electrically conducting fluids over surfaces of a magnetic field in recent years. The interest is due to the extensive use of these fluids in various geophysical and industrial applications.

The advent of technology in the field of Magnetohydrodynamic (MHD) power generators and Magnetohydrodynamic (MHD) devices, nuclear engineering and thermonuclear power has a great practical need for understanding the dynamics of conducting fluids. The use of liquid metals as heat transfer agents and as working fluids in Magnetohydrodynamic (MHD) power generators has created a growing interest in the study of liquid metal flows and magnetic field which radically modifies the flow and heat transfer characteristics.

Several investigators have conducted various research works on the unsteady magneto hydrodynamic (MHD) free convection flow in a vertical channel. Chen and Weng (2005) investigated the fully developed natural convection in vertical parallel plate micro-channels due to heating of channel walls. Their result reveals that the effect of rarefaction and fluid-wall interaction increases the volume flow rate, while it decreases the rate of heat transfer. This result is further extended by taking into account suction/injection on the micro-channel walls by Jha *et.al* (2013). They concluded that skin-friction as well as the rate of heat transfer strongly depends on the suction/injection parameter.

Micro-electro-mechanical systems (MEMS) and nano-electro-mechanical systems (NEMS) have received great interest in recent years. These highly integrated systems are now widely applied to various applications. As a basic element in MEMS/NEMS devices, micro-channel is often found to be used for integrated cooling or heating in micro-reactor devices. Current

applications of such devices include micro-channel heatsink, microjet impingement cooling and micro heat pipe.

Most of these proposed designs involve internal micro-channel flows. Therefore, a thorough understanding of the flow behaviors in micro-channel is becoming increasingly important for accurate prediction of performance during the design process. Although there are remarkably growing number of realized scientific and engineering applications found for MEMS devices, the understanding on the fluid dynamics and heat transfer processes in such MEMS devices is still far from being thorough. On one hand, the performance of MEMS often defies predictions made using scaling laws developed for large systems. On the other hand, heat can be easily built up in a densely packed MEMS protective housing, which may cause undesirable or even destructive deformation. Therefore, there is a pressing need of reliable computational capabilities for accurate predictions of these devices.

The key quantity in micro-channel analysis is Knudsen number (Kn), defined as the ratio of molecular mean free path to the characteristic length ($Kn = \lambda/b$). Knudsen number is very small for continuum flows. However, for micro-scale gas flows where the gas mean free path becomes comparable with the characteristic dimension of the duct, the Knudsen number may be greater than 10^{-3}. Micro-channel with characteristic lengths on the order of $100\mu m$ would produce flows inside the slip regime for gas with a typical mean free path of approximately $100\mu m$ standard condition. Some of the slip flow studies in micro-channels are summarized here. Yu and Ameel (2001) studied slip flow heat transfer in micro-channels and found that heat transfer increases, decreases, or remains unchanged, compared to no-slip flow conditions, depending on two dimensionless variables that include effects of rarefaction and the fluid/wall interaction.

A series of investigations have been conducted recently in the field of micro geometry flow. However, to cite a few works in this direction, Chen and Weng (2005) analytically studied the fully developed natural convection in opened-ended vertically parallel plate micro-channels with asymmetric wall temperature distribution in which the effect of rarefaction and fluid wall interaction was shown to increase the volume flow rate and decrease the heat transfer. In another article, Larrode *et al.* (2000) and Yu and Ameel (2001) considered the temperature jump condition and found that the effect of fluid-wall interaction is very important. The effect of hyberbolic heat conduction model on the transient hydrodynamics and thermal behaviours of fluid flow in an open-ended vertical parallel plate micro-channel was analytically studied by Khadrawi *et al*. (2005). Biswal *et al*. (2007) numerically investigated the flow and heat transfer characteristics in the developing region of an isothermal planar micro-channel by using the semi-implicit method for pressure linked equations. Chen and Weng (2005) model the developing convection in an asymmetrically heated planar micro-channel based on the second-order Beskok-Karniadakis slip/jump boundary conditions by using a marching implicit procedure.

In order to have a confident study of this nature, this chapter therefore, explains some of the related literature of some previous researches and attempts to review and discuss them in two parts as in section 2.1 and 2.2.

2.1 MHD Natural Convection Flow in Vertical Parallel Plate Micro-channels

The flow of eclectically conducting fluid through a channel or circular pipe in the presence of transverse magnetic field is encountered in a variety of applications such as Magnetohydrodynamic (MHD) generators, pumps, accelerators and flow meters. Besides these applications, when the fluid is electrically conducting, the free convection flow is appreciably influenced by an imposed magnetic field. Also the advent of technology in the

field of Magnetohydrodynamic (MHD) power generators and Magnetohydrodynamic (MHD) devices, nuclear engineering and thermonuclear power has created a great practical need for understanding the dynamics of conducting fluids. The use of liquid metals as heat transfer agents and as working fluids in Magnetohydrodynamic (MHD) power generators has created a growing interest in the study of liquid metal flows and magnetic field radically modifies the flow and heat transfer characteristics.

Several investigators have conducted much research work on the unsteady Magneto hydrodynamic (MHD) free convection flow in a vertical channel. In the past, several MHD free convection flow solutions were obtained by Crammer and Pai (2006), Chawlar (1967), Soundalgekar and Takhar (1977) and so on. Sheikholeslamia *et al*. (2014) investigated the magnetic field effect on nanofluid flow and heat transfer in a semi-annulus enclosure via control volume-based finite element method. Sheikholeslamia and Gorji-Bandpy (2014) presented the numerical solution for free convection of ferrofluid in a cavity heated from below in the presence of external magnetic field, while the magnetohydrodynamic natural convection of nanofluid in a concentric annulus between a cold outer square cylinder and a heated inner circular is investigated by Sheikholeslamia *et al*. (2014).

Some recent works related to the present investigation found in literature of Sheikholeslamia *et al*. (2014) conducted a numerical investigation of MHD natural convection heat transfer in an L-shape inclined enclosure filled with nanofluid. Sheikholeslamia *et al*. (2014) studied the magnetohydrodynamic effect on natural convection heat transfer of Cu-water nanofluid in an enclosure with hot elliptic cylinder. Also, Sheikholeslamia *et al*. (2012) numerically examined the natural convection of nanofluids in a concentric annulus between a cold outer square cylinder and a heated inner circular. Flow and heat transfer of a nanofluid over a stretching cylinder in the presence of magnetic field has been investigated by Ahorynejad *et*

al. (2013). Recently, Sheikholeslamia *et al*. (2012) presented the numerical solution for natural convection of nanofluids in cold outer circular enclosure containing a hot inner sinusoidal cylinder. Sheikholeslamia *et al*. (2013) carried out a numerical investigation on natural convection nanofluid in a half annulus enclosure with one wall under constant heat flux in the presence of magnetic field. In another work, Control-Based Finite Element Method (CBFEM) was applied to investigate flow and heat transfer of Cu-water nanofluid in the presence of magnetic field by Sheikholeslamia *et al*. (2014); and so on. However, derivation of any closed form analytical expression for MHD natural convection flow in a vertical micro-channel with interfacial slip has not been attempted. It can be mentioned in this respect that besides their theoretical as well as archival implication, such analytical solutions also hold the potential for assessing the accuracy, convergence and effectiveness of various numerical computation methods employed for solving Magnetohydrodynamic (MHD) natural convection flow in vertical micro-channel problems with slip. With the aid of such close formed solutions, the characteristics of the whole solution can be grasped easily. Thus, closed-form solutions for Magnetohydrodynamic (MHD) natural convection flow in a vertical micro-channel problem with interfacial slip is not only expected to contribute towards the development of archival literature, but also holds the potential of accomplishing the task for efficient design of microfluidic system devices. In all these works above, there was none that considered the fully developed steady natural convection flow of conducting fluid in vertical parallel plate micro-channel in the presence of transverse magnetic field, hence the motivation of this work.

The main goal of the present work is to investigate the influence of externally applied transverse magnetic field on steady natural convection flow of conducting fluid in vertical micro-channels. The effect of rarefaction parameter, fluid-wall interaction parameter, and Hartmann number are discussed with the aid of line graphs. The present work extends the

work of Chen and Weng (2005) by considering the influence of externally applied transverse magnetic field on steady natural convection flow of conducting fluid in vertical micro-channels.

2.2 Suction/Injection on MHD Natural Convection in Vertical Parallel Plate Micro-channels

Suction or injection of fluid through the bounding surfaces, as, for example, in mass transfer cooling, can significantly change the flow field and consequently affect the rate of heat transfer from the bounding surfaces. In general, suction tends to increase the skin-friction and heat transfer co-efficient whereas injection acts in the opposite manners. Injection or withdrawal of fluid through porous heated or cooled surface is of general interest in practical problems involving film cooling, control of boundary layers, etc. This can lead to enhanced heating (or cooling) of the system and can help to delay the transition of laminar flow.

The significance of suction/injection on the boundary layer control in the field of aerodynamics and space science is well recognized. One of the early studies on natural convective gas microflow was analytically studied by Chen and Weng (2005) for the fully developed natural convection in vertical parallel plate micro-channels with asymmetric wall temperature distributions. The effect of rarefaction and fluid-wall interaction were shown to increase the flow rate and decrease the heat transfer rate. This result is further extended by taking into account suction/injection on the micro-channel walls by Jha *et al*. (2013). They concluded that skin-friction as well as rate of heat transfer strongly depends on the suction/injection parameter. Singh (1984) and Ishak *et al.* (1968) showed that suction/injection of a fluid through the bounding surface, for instance, in mass transfer cooling, can significantly change the flow field and, as a consequence, affect the heat transfer rate of plate. Also, Al-Sanea (2004) pointed out that in general, suction tends to increase the skin friction and heat transfer coefficient, whereas injection acts in the opposite manner.

Suction/injection plays an important role in the control of flow past an infinite plate or within parallel plates; hence, its importance in practical problems involving film cooling, control of boundary layers in industrial, geophysical, biomedical, engineering and environmental applications. Khadrawi *et al*. (2005) studied the transient hydrodynamics and thermal behaviours of fluid flow in an open-ended vertical parallel plate micro-channel under the effect of hyperbolic heat conduction model. Also, Hadded *et al*. (2005) numerically investigated the developing hydrodynamic behaviours of free convective gas flow in a vertical open-ended parallel plate micro-channel filled with porous media. Biswal *et al.* (2007) investigated the flow and heat transfer characteristic in the developing region of a micro-channel by using the Semi-Implicit Method for Pressure Linked Equations (SIMPLE) and concluded that the microscale effects associated with the velocity slip and the temperature jump enhances the heat transfer. Al-jarrah *et al*. (2008) discussed the effects of the velocity and temperature slip on film condensation in micro-channel between two vertical plates.

The work herein investigates the combined influence of externally applied transverse magnetic field and suction/injection on steady natural convection flow of conducting fluid in vertical micro-channels. The method of undetermined coefficient is employed to obtain the closed-form solutions for the present mathematical model. The influences of rarefaction parameter, fluid-wall interaction parameter, suction/injection parameter and Hartmann number on the flow are investigated. This work extends the work of Jha *et al.* (2013) by considering the influence of externally applied transverse magnetic field on steady natural convection flow of conducting fluid in vertical micro-channels.

The methodology followed herein is described in chapter three.

CHAPTER THREE

MATHEMATICAL ANALYSIS AND METHOD OF SOLUTIONS

3.0 Introduction

This chapter is concerned with the derivation of velocity and temperature equations and their solutions. The non-dimensional equations are derived from the dimensional equations using appropriate non-dimensional parameters.

3.1 MHD Natural Convection Flow in Vertical Parallel Plate Micro-channels

The objective here in this chapter is to study the impact of transverse magnetic field on Magnetohydrodynamic (MHD) natural convection flow in vertical parallel plate micro-channels.

3.1.1 Mathematical Analysis

The fully developed steady natural convection flow of viscous, incompressible, electrically conducting fluid in micro-channels formed by two vertical plates under the effect of transverse magnetic field is considered. The x-axis is parallel to the gravitational acceleration, g, but in the opposite direction while the y-axis is orthogonal to the vertical parallel plates. A magnetic field of uniform strength $(0, \boldsymbol{B_0}, 0)$ is assumed to be applied in the direction perpendicular to the direction of flow. It is also assumed that the magnetic Reynolds number is very small, which corresponds to negligibly induced magnetic field compared to the externally applied one. The plates are heated asymmetrically with one plate maintained at a temperature, T_1, while the other plate is at a temperature, T_2, where $T_1 > T_2$. Due to this temperature gradient between the plates, natural convection flow occurs in the channel. The geometry of the system under consideration in this present study is shown schematically in Figure 3.1.

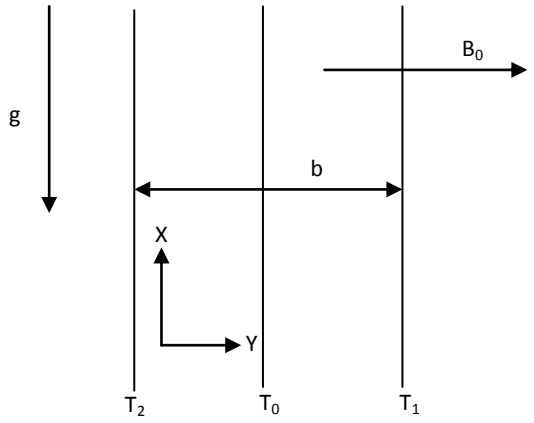


Figure 3.1: Flow configuration and coordinate system of the first problem.

Thus under the usual Boussinesq's approximation, the governing momentum and energy equations can be written in dimensional form as follows:

$$\nu \frac{d^2u}{dy^2} + g\beta(T - T_0) - \frac{\sigma B_0^2 u}{\rho} = 0 \tag{3.1}$$

$$\frac{d^2T}{dy^2} = 0 \tag{3.2}$$

The boundary conditions which describe velocity slip and temperature jump conditions at the fluid wall interface in dimensional form are:

$$u(y=0) = \frac{2 - f_v}{f_v} \lambda \left.\frac{du}{dy}\right|_{y=0} \tag{3.3}$$

$$u(y=b) = -\frac{2 - f_v}{f_v} \lambda \left.\frac{du}{dy}\right|_{y=b} \tag{3.4}$$

$$T(y=0)=T_2+\frac{2-f_t}{f_t}\frac{2\gamma}{\gamma+1}\frac{\lambda}{\Pr}\frac{dT}{dy}\bigg|_{y=0} \tag{3.5}$$

$$T(y=b)=T_1-\frac{2-f_t}{f_t}\frac{2\gamma}{\gamma+1}\frac{\lambda}{\Pr}\frac{dT}{dy}\bigg|_{y=b} \tag{3.6}$$

3.2 Suction/Injection on MHD Natural Convection in Vertical Parallel Plate Micro-channels

The objective is to study the role of suction/injection on Magnetohydrodynamic (MHD) natural convection flow in vertical parallel plates micro-channels.

3.2.1 Mathematical Analysis

The flow considered is a fully developed steady natural convection flow of viscous, incompressible, electrically conducting fluid in micro-channels formed by two vertical porous plates under the effect of transverse magnetic field as presented in Figure 3.2. The x-axis is parallel to the gravitational acceleration, g, but in the opposite direction, while the y-axis is orthogonal to the vertical parallel plates. A magnetic field of uniform strength $(0, \boldsymbol{B_0}, 0)$ is assumed to be applied in the direction perpendicular to the direction of flow. It is assumed that the magnetic Reynolds number is very small, which corresponds to negligibly induced magnetic field compared to the externally applied one. Fluid is being injected into the flow region through the cold porous plate and in order to conserve the mass of the fluid in the channel, fluid is being sucked out of the channel at the same rate through the hot porous plate. In addition, the plates are heated asymmetrically with one plate maintained at a temperature, T_1, while t6he other plate is at a temperature, T_2, where $T_1 > T_2$. Due to this temperature gradient between the two porous plates, natural convection flow occurs in the channel.

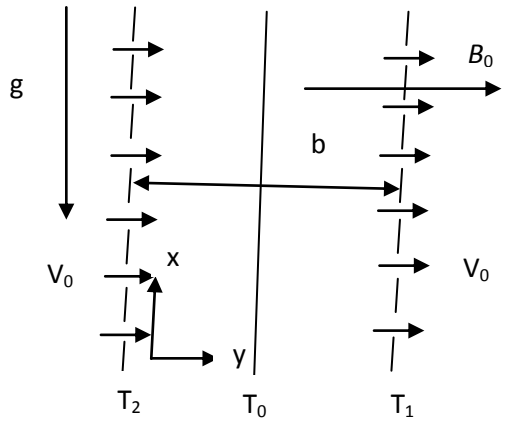


Figure 3.2: Flow configuration and coordinate system of the second problem.

Thus under the usual Boussinesq's approximation, the governing momentum and energy equations can be written in dimensional form as follows:

$$V_0 \frac{du}{dy} = \nu \frac{d^2u}{dy^2} + g\beta(T - T_0) - \frac{\sigma B_0^2 u}{\rho} \tag{3.7}$$

$$V_0 \frac{dT}{dy} = \frac{k}{\rho C_\rho} \frac{d^2T}{dy^2} \tag{3.8}$$

The boundary conditions which describe velocity slip and temperature jump conditions at the fluid wall interface in dimensional form are:

$$u(y=0) = \frac{2 - f_v}{f_v} \lambda \left.\frac{du}{dy}\right|_{y=0} \tag{3.9}$$

$$u(y=b) = -\frac{2 - f_v}{f_v} \lambda \left.\frac{du}{dy}\right|_{y=b} \tag{3.10}$$

$$T(y=0) = T_2 + \frac{2 - f_t}{f_t} \frac{2\gamma}{\gamma + 1} \frac{\lambda}{\mathrm{Pr}} \left.\frac{dT}{dy}\right|_{y=0} \tag{3.11}$$

$$T(y=b) = T_1 - \frac{2 - f_t}{f_t} \frac{2\gamma}{\gamma + 1} \frac{\lambda}{\mathrm{Pr}} \left.\frac{dT}{dy}\right|_{y=b} \tag{3.12}$$

3.3 Non Dimensionalisation

In engineering, the application of fluid mechanics in designs makes much use of empirical results from a lot of experiments. These results are presented in dimensional form. Dimensional analysis provides a strategy for choosing relevant data and how they should be presented. This is a useful technique in all experimentally based areas in engineering. If it is possible to identify the factors involved in a physical situation, dimensional analysis can form a relationship between them. The result data obtained are often difficult to present in a readable form. Even from graphs they may be difficult to interpret. Therefore, these qualitative results, when converted to quantitative forms can be used to obtain any unknown factor from experimental analysis. So the governing equations of the above problems in dimensional form are non-dimensionalised to obtain their non-dimensional form.

The governing equations (3.1) and (3.2) in dimensional form with boundary conditions (as stated in Equations (3.3) to (3.6)) are non-dimensionalised using the non-dimensional parameters in Equation (3.13) below.

$$Y = \frac{y}{b},\ \theta = \frac{T_T_0}{T_1 - T_o},\ U = \frac{u}{U_0},\ M^2 = \frac{\sigma B_0^2 b^2}{\rho \nu} \tag{3.13}$$

$$Pr = \frac{\nu}{\alpha},\ S = \frac{V_0 b}{\nu},\ \text{where}\ U_0 = \frac{\rho g \beta\ (T_1 - T_o) b^2}{\mu}.$$

By substituting Equation (3.13) into equations (3.1) to (3.6), we have the momentum and energy equations presented in dimensionless form as

$$\frac{d^2U}{dY^2} - M^2 U + \theta = 0 \tag{3.14}$$

and

$$\frac{d^2\theta}{dY^2} = 0. \tag{3.15}$$

The boundary conditions which describe velocity slip and temperature jump conditions at the fluid – wall interface are:

$$U(0) = \beta_v Kn \frac{dU}{dY}\Big|_{Y=0},\ U(1) = -\beta_v Kn \frac{dU}{dY}\Big|_{Y=1}$$

$$\theta(0) = \xi + \beta_v Knln \frac{d\theta}{dY}\Big|_{Y=0},\quad \theta\,(1) = 1 - \beta_v Knln \frac{d\theta}{dY}\Big|_{Y=1} \tag{3.16}$$

The governing Equations (3.7) and (3.8) in dimensional form with boundary conditions (as given in Equations (3.9 to 3.12)) are non-dimensionalised using the non-dimensional parameters in Equation (3.13).

By substituting Equation (3.13) into Equations (3.7) to (3.12), we have the momentum and energy equations presented in dimensionless form as

$$\frac{d^2U}{dY^2} - S\frac{dU}{dY} - M^2U + \theta = 0 \tag{3.17}$$

and

$$\frac{d^2\theta}{dY^2} - SPr\frac{d\theta}{dY} = 0. \tag{3.18}$$

The boundary conditions which describe velocity slip and temperature jump conditions at the fluid – wall interface are:

$$U(0) = \beta_v Kn \frac{dU}{dY}\Big|_{Y=0},\ U(1) = -\beta_v Kn \frac{dU}{dY}\Big|_{Y=1}$$

$$\theta(0) = \xi + \beta_v Knln \frac{d\theta}{dY}\Big|_{Y=0},\quad \theta\,(1) = 1 - \beta_v Knln \frac{d\theta}{dY}\Big|_{Y=1} \tag{3.19}$$

where:

$$\beta_v = \frac{2-f_v}{f_v},\ \beta_t = \frac{2-f_t}{f_t}\frac{2\gamma_s}{\gamma_s+1}\frac{1}{Pr},\ Kn = \frac{\lambda}{b},\ ln = \frac{\beta_t}{\beta_v},\ \xi = \frac{T_2-T_o}{T_1-T_o}.$$

Here γ_s is the ratio of specific heats, Pr is the Prandtl number, f_v and f_t are the tangential momentum and thermal accommodation coefficients, respectively, and range from near 0 to 1, λ is the molecular mean free path, Kn is the Knudsen number, ln is the fluid – wall interaction parameter, and ξ is the wall- ambient temperature difference ratio. Referring to the values of f_v and f_t given in Eckert and Drake (1972) and Goniak and Duffa (1995), the value of β_v is near unity, and the value of β_t ranges from near 1 to more than 100 for actual wall surface conditions and is near 1.667 for many engineering applications, corresponding to $f_v = 1.0; f_t = 1.0; \gamma_s = 1.4$ and $Pr = 0.71$ ($\beta_v = 1.0;\ \beta_t = 1.667$).

3.4 Solution to Problems

The dimensionless equations derived in this chapter are solved by the method of undetermined coefficient.

3.4.1 Solution to MHD Natural Convection Flow in Vertical Parallel Plates Micro-channels

Equations (3.14) and (3.15), subject to the boundary conditions, (3.16) have the following exact solutions:

$$\theta(Y) = A_0 + A_1(Y) \tag{3.20}$$

$$U(Y) = A_2 exp(MY) + A_3 exp(-MY) + \frac{A_0}{M^2} + \frac{A_1 Y}{M^2} \tag{3.21}$$

where:

$A_0 = \xi + \frac{\beta_v \mathrm{KnIn}\ (1-\xi)}{1+2\beta_v \mathrm{KnIn}},\ A_1 = \frac{1-\xi}{1+2\beta_v \mathrm{KnIn}}, A_2 = F_5 - \frac{\beta_v \mathrm{KnM}\ F_7}{F_4 F_6} - \frac{F_7}{F_4 F_6}$, and $A_3 = \frac{F_7}{F_6}$

Two important parameters for buoyancy – induced microflow and microheat transfer are the volume flow rate, m, and heat transfer rate, q, respectively. The dimensionless volume flow rate is:

$$Q = \frac{m}{bU_0} = \int_0^1 UdY \tag{3.22}$$

Substituting Equation (3.21) into equation (3.22), we obtain

$$Q = \frac{A_2 \exp(M)}{M} - \frac{A_3 \exp(-M)}{M} + \frac{A_0}{M^2} + \frac{A_1}{SPrF_3} - \frac{A_2}{M} + \frac{A_3}{M} \tag{3.23}$$

Also the rate of heat transfer which is expressed as the Nusselt number are:

$$Nu = \frac{qb}{(T_1 - T_0)k} = \frac{d\theta}{dY}\Big|_{Y=0} = \frac{d\theta}{dY}\Big|_{Y=1} = A_1 \tag{3.24}$$

Using Expression (3.21), we obtain the skin - friction (τ) on the micro-channel plates as follows:

$$\tau_0 = \frac{dU}{dY}\Big|_{Y=0} = MA_2 - MA_3 + F_3 \tag{3.25}$$

$$\tau_1 = \frac{dU}{dY}\Big|_{Y=1} = MA_2 \exp(M) - MA_3 \exp(-M) + F_3 \tag{3.26}$$

All the constants are declared in Appendix I

3.4.2 Solution to Suction/Injection on MHD Natural Convection in Vertical Parallel Plate Micro-channels

Equations (3.17) and (3.18), subject to the boundary conditions, (as in Equation (3.19)) have the following exact solutions:

$$\theta(Y) = A + Bexp(SPrY) \tag{3.27}$$

$$U(Y) = Cexp(K_1 Y) + Dexp(K_2 Y) + \frac{A}{M^2} - \frac{Bexp\,(SPrY)}{F_3} \tag{3.28}$$

where:

$A = \frac{F_2}{F_1}$, $B = \frac{(1-\xi)}{F_1}$, $C = \frac{\beta_v Kn K_2 F_{11}}{F_9 F_{10}} - \frac{F_{11}}{F_9 F_{10}} + \frac{F_8}{F_9}$, and $D = \frac{F_{11}}{F_{10}}$

Two important parameters for buoyancy – induced microflow and microheat transfer are the volume flow rate, m, and heat transfer rate, q, respectively. The dimensionless volume flow rate is:

$$Q = \frac{m}{b U_0} = \int_0^1 U dY \tag{3.29}$$

Substituting Equation (3.28) into Equation (3.29), we do obtain

$$Q = \frac{Cexp\,(K_1)}{K_1} + \frac{Dexp\,(K_2)}{K_2} + \frac{A}{M^2} - \frac{Bexp\,(SPr)}{SPr\,F_3} - \frac{C}{K_1} - \frac{D}{K_2} + \frac{B}{SPr\,F_3} \tag{3.30}$$

Also the rate of heat transfer which is expressed as the Nusselt number is

$$Nu = \frac{qb}{(T_1 - T_0)k} = \frac{d\theta\,(Y)}{dY} = B(SPr)\exp(SPrY)$$

Therefore:

$$Nu_0 = \frac{d\theta}{dY}\Big|_{Y=0} = BSPr \tag{3.31}$$

$$Nu_1 = \frac{d\theta}{dY}\Big|_{Y=1} = BSPr\ exp(SPr) \tag{3.32}$$

Using expression (3.28), we obtain the skin - friction (τ) on the channel plates as follows:

$$\tau_0 = \frac{dU}{dY}\Big|_{Y=0} = CK_1 + DK_2 - F_6 \tag{3.33}$$

$$E = \frac{dU}{dY}\Big|_{Y=1} = CK_1\exp(K_1) + DK_2\exp(K_2) - F_7 \tag{3.34}$$

All the constants are defined in Appendix II.

CHAPTER FOUR

RESULTS AND DISCUSSIONS

4.0 Introduction

This chapter gives the results and discussions of the solutions to the problems as earlier noted in sections (3.4.1) and (3.4.2).

To see the physical impact of the Hartmann number, rarefaction parameter, and fluid-wall interaction parameter on the flow, we have plotted the line graphs for velocity, volume flow rate and skin-friction. The present parametric study has been performed over reasonable ranges of $0 \leq \beta_v Kn \leq 0.1$, $0 \leq$ M ≤ 2 and $0 \leq ln \leq 10$. The product of $\beta_v Kn$ represents a measure of the departure from the continuum regime, while ln represents a property of the fluid – wall interaction. The selected reference values of $\beta_v Kn$, and ln for the analysis are 0.05 and 1.667 as presented by Chen and Weng (2005). In addition, the values of Hartmann number (M) are taken over the range of $0 \leq M \leq 2$ with a reference value of $M = 2$.

The expression for the temperature in Equation (3.5), effects of the rarefaction parameter $(\beta_v Kn)$, and fluid-wall interaction parameter (ln) on the temperature profile and rate of heat transfer, which is expressed as the Nusselt number are exactly the same as those given by Chen and Weng (2005).

4.1 Results for MHD Natural Convection Flow in Vertical Parallel Plates Micro-channels

Figure 4.1.1 shows the velocity variation for different values of rarefaction parameter $(\beta_v Kn)$. It is observed that as $\beta_v Kn$ increases, the velocity slip at the wall increases, which reduces the retarding effect of the wall. This yields an observable increase in the gas velocity near the wall. In addition, as the wall-ambient temperature difference ratio (ξ) increases, the

effect of rarefaction parameter ($\beta_v Kn$) on the micro-channels slip velocity becomes significant.

Figure 4.1.2 shows the velocity variation for different values of fluid – wall interaction parameter (ln). It clearly reveals that velocity slip increases on the micro-channels surfaces with increases of fluid wall interaction parameter, while the impact of fluid-wall interaction parameter on the micro-channels slip velocity become significant with the decreases in the wall-ambient temperature difference ratio (ξ).

Figure 4.1.3 shows the velocity variation for various values of Hartmann number (M). It is found from Figure 4.1.3 that the effect of the Hartmann number is to decrease the fluid velocity. This is the classical Hartmann effect. Furthermore, the effect of Hartmann number on the micro-channel slip velocity becomes significant with increases in the wall-ambient temperature difference ratio (ξ).

The variation of volume flow rate are displayed in Figure 4.1.4 with respect to fluid-wall interaction parameter (ln) and the departure from the continuum regime ($\beta_v Kn$) for different values of wall-ambient temperature difference ratio (ξ). It is obvious from Figure 4.1.4,that increasing $\beta_v Kn$ yields corresponding increase in volume flow rate whenever $ln = 0$, regardless of ξ, but with $ln > 0$ increasing $\beta_v Kn$ yields decreases in volume flow rate and this physically true since increasing $\beta_v Kn$ yields increases in velocity as shown in Figure 4.1.1. It is interesting to note that as the value of wall – ambient temperature difference ratio (ξ) increases, there are decreases in the volume flow.

Figure 4.1.5 presents variation of volume flow rate with respect to Hartmann number (M) and the departure from the continuum regime ($\beta_v Kn$) for various values of wall-ambient temperature difference ratio (ξ). From this figure, it is observed that as Hartmann number

(M) increases, the volume flow rate decrease. This is due to the fact that, as the Hartmann number increases, the velocity decreases. It is also interesting to note that the effect of Hartmann number is minimized for the case of symmetric heating ($\xi = 1$).

The variation of skin-friction are revealed in Figures 4.1.6 and 4.1.7 with respect to fluid-wall interaction parameter (ln) and the departure from the continuum regime ($\beta_v Kn$) for various values of wall-ambient temperature difference ratio (ξ) at the micro-channel plates, $Y = 0$ and $Y = 1$, respectively. It is observed from these figures that the skin-friction increases with increases in the values of fluid – wall interaction parameter (ln). Further, it is found that the impact of fluid-wall interaction parameter (ln) is insignificant for symmetric heating of micro-channel plates ($\xi = 1$).

Figures 4.1.8 and 4.1.9 show the combined effects of Hartmann number (M) and the departure from the continuum regime ($\beta_v Kn$) for various values of wall-ambient temperature difference ratio (ξ) at the micro-channel plates $Y = 0$ and $Y = 1$, respectively. It is evident from these figures that the skin-friction decreases with increases in the values of Hartmann number (M) at $Y = 0$ while the reverse phenomenon occurs at $Y = 1$. In addition, the magnitude of skin-friction is higher in the case of symmetric heating ($\xi = 1$) in comparison to asymmetric heating of micro-channel plates ($\xi = 0$).

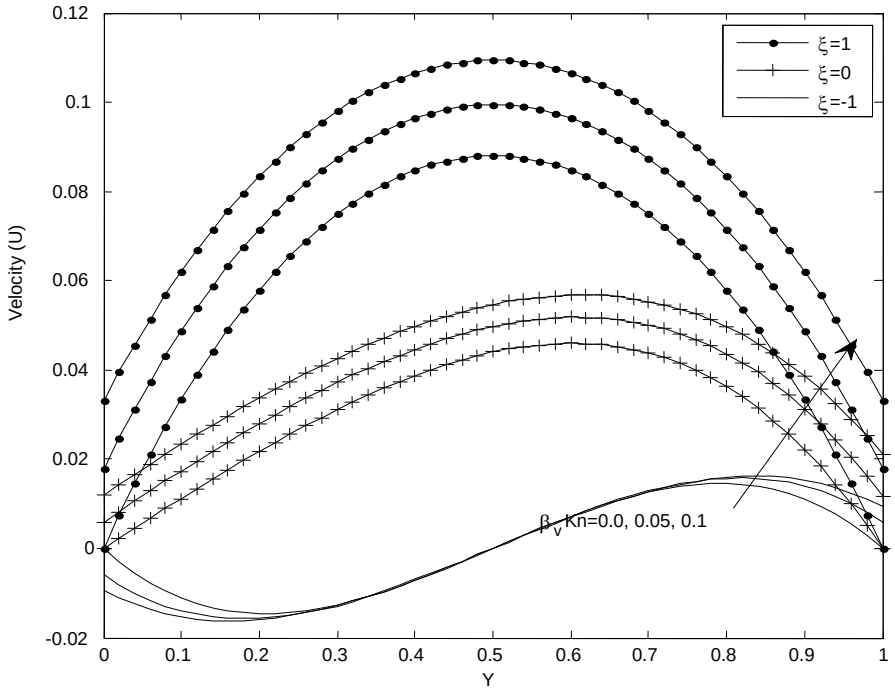


Figure 4.1.1: Velocity profile for various values of $\beta_v Kn$ ($ln = 1.667$, $M = 2.0$)

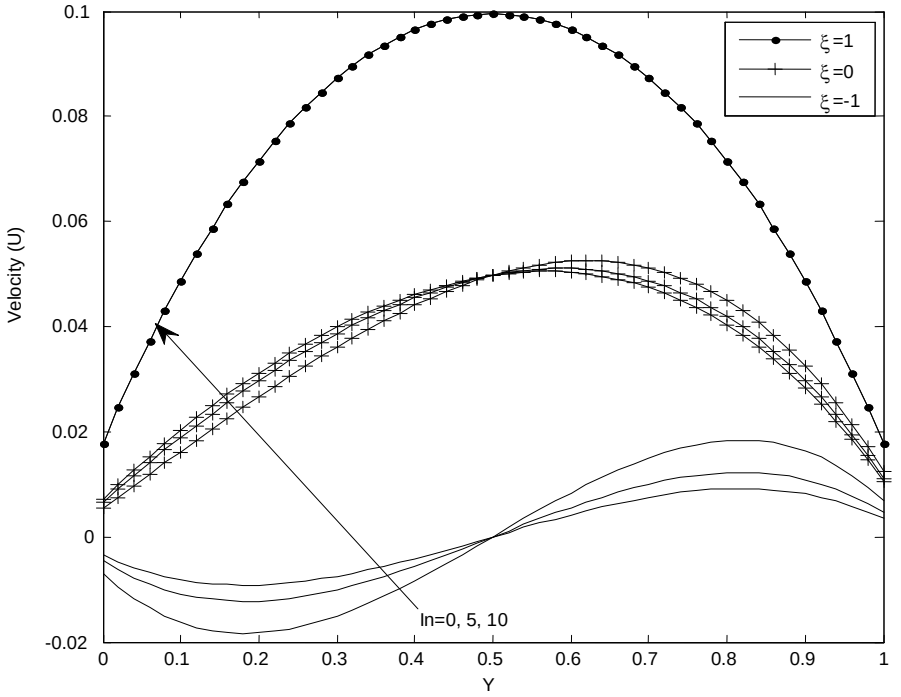


Figure 4.1.2: Velocity profile for various values of ln ($\beta_v Kn = 0.05$, $M = 2.0$)

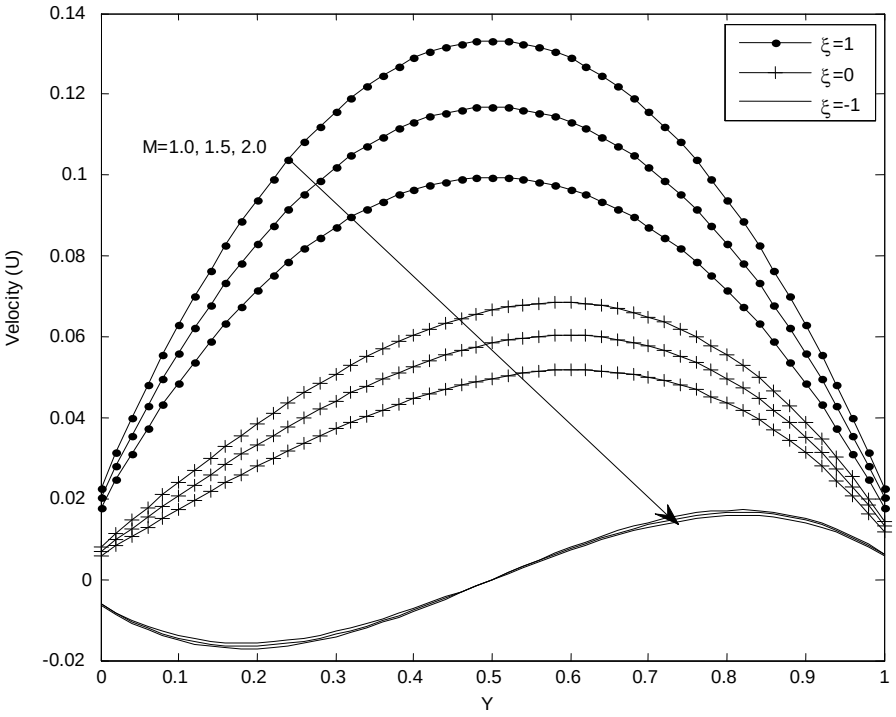


Figure 4.1.3: Velocity profile for various values of *M* ($\beta_v Kn = 0.05$, $ln = 1.667$)

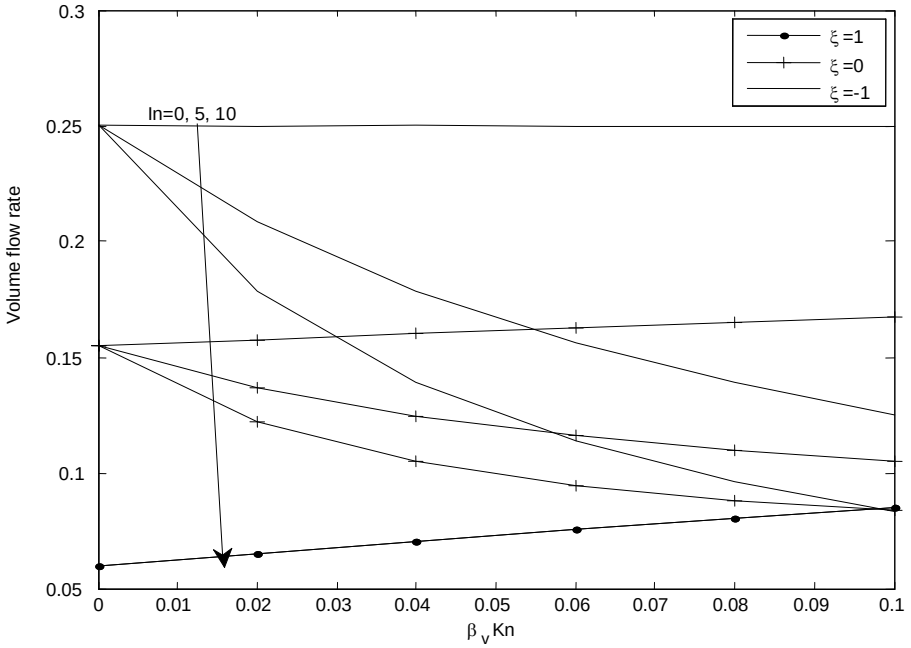


Figure 4.1.4: Relationship of Volume flow rate to $\beta_v Kn$ for various values of *ln*

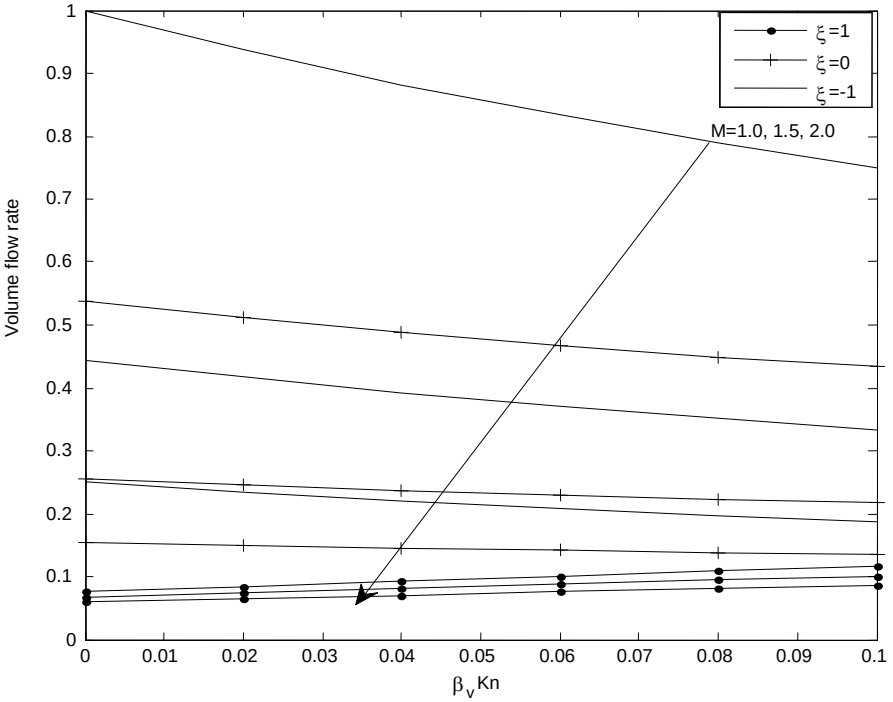


Figure 4.1.5: Relationship of Volume flow rate to $\beta_v Kn$ for various values of *M*

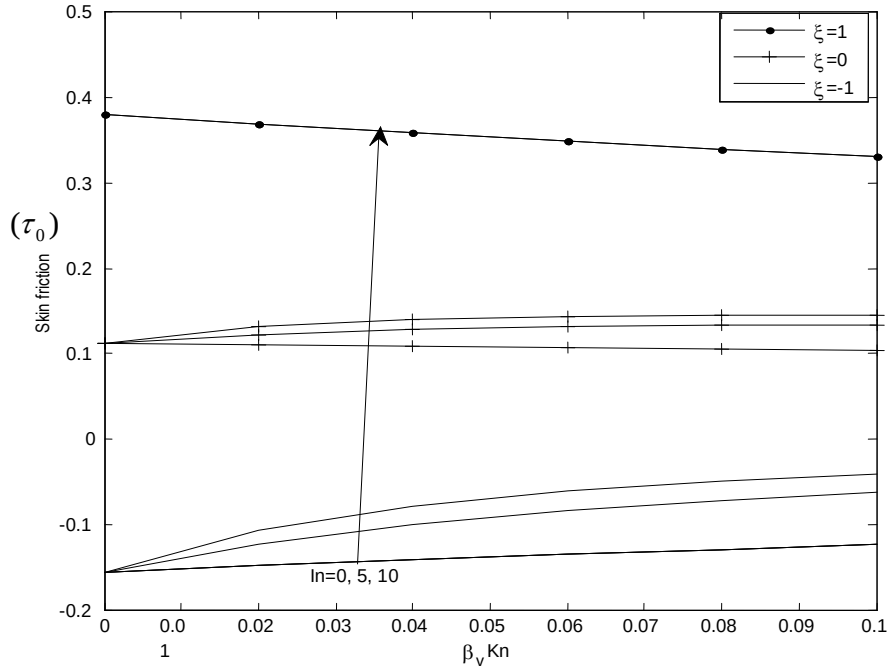


Figure 4.1.6: Relationship of skin friction to various values of *In* (*Y = 0*)

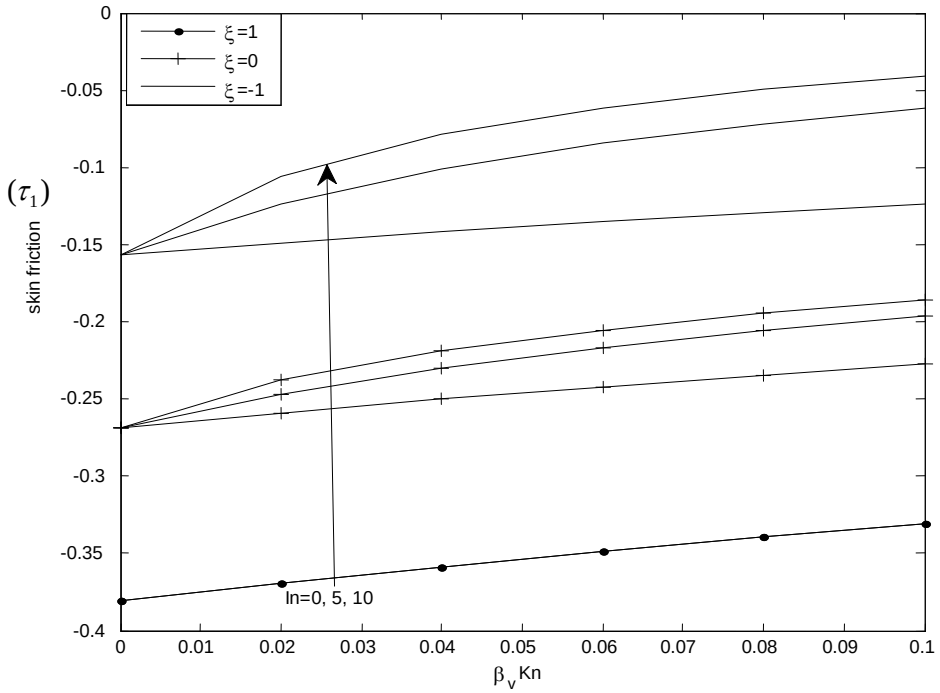


Figure 4.1.7: Relationship of skin friction to various values of *ln* (*Y = 1*)

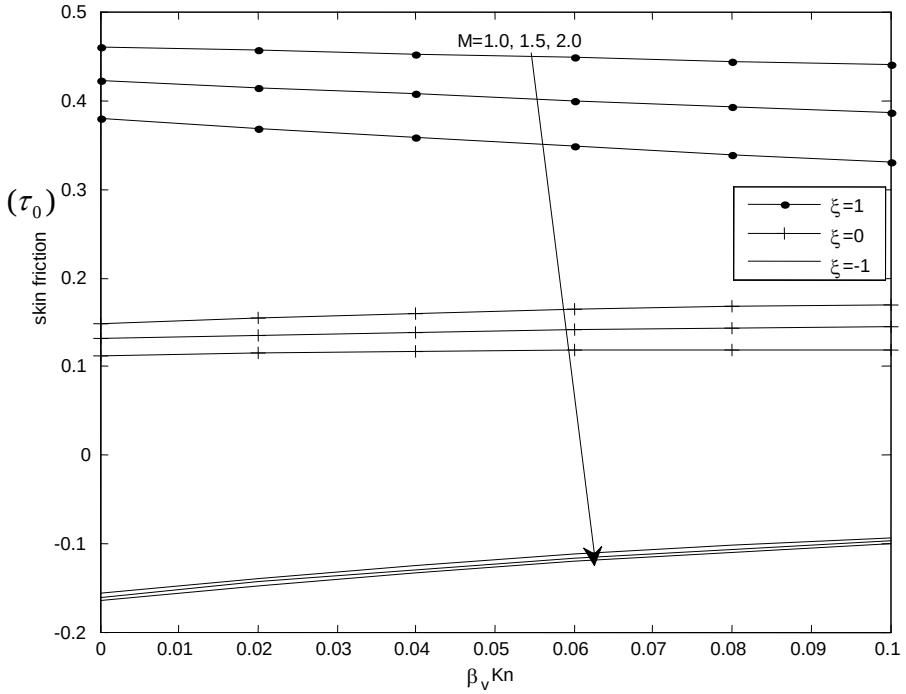


Figure 4.1.8: Relationship of skin friction to various values of *M* (*Y = 0*)

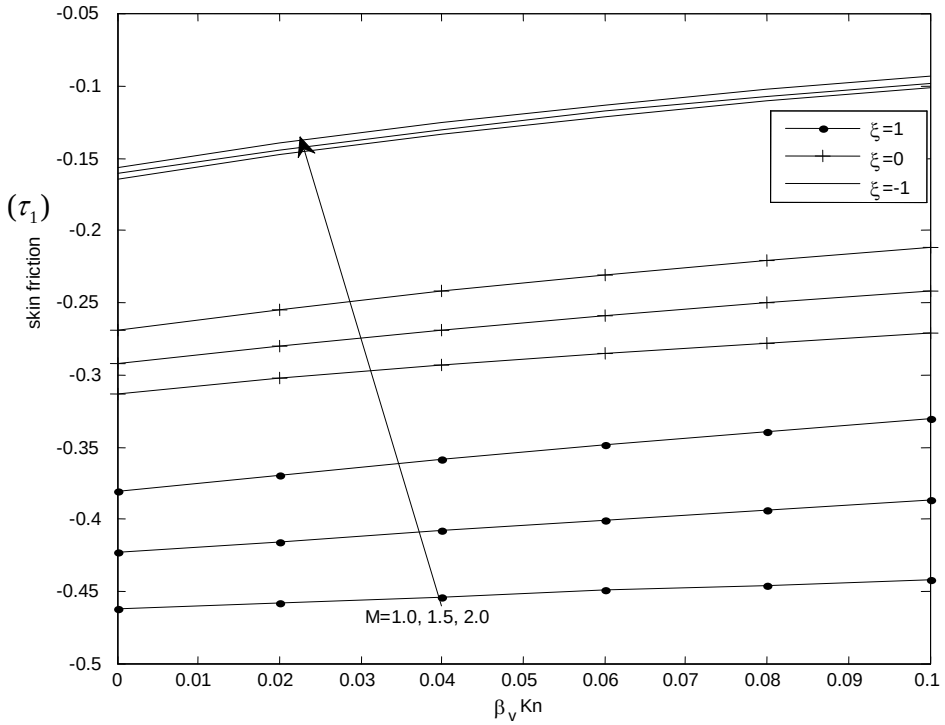


Figure 4.1.9: Relationship of skin friction to various values of *M* (*Y = 1*)

4.2 Results for Suction/Injection on MHD Natural Convection in Vertical Parallel Plate Micro-channels

Figure 4.2.1 shows the velocity variation for various values of rarefaction parameter ($\beta_v Kn$). It is clear from this Figure 4.2.1, that as $\beta_v Kn$ increases, the velocity slip at the wall increases which reduce the retarding effect of the wall. This yields observable increases in the gas velocity near the wall. Further, as $\beta_v Kn$ increases, the temperature jump increases and reduces the amount of heat transfer from the wall to the fluid. This reduction in heat transfer reduces the buoyancy effect, which derives the flow and hence, reduces the gas velocity far from the wall. In addition, as the wall-ambient temperature difference ratio (ξ) increases, the effect of rarefaction parameter ($\beta_v Kn$) on the micro-channels slip velocity becomes significant.

Figure 4.2.2 shows the velocity variation for various values of fluid-wall interaction parameter (ln). It is clearly revealed that velocity slip increases on the micro-channels surfaces with increases in fluid wall interaction parameter. Furthermore, the effect of fluid-

wall interaction parameter (ln) on the micro-channels slip velocity becomes significant for small values of wall – ambient temperature difference ratio (ξ).

Figure 4.2.3 shows the velocity variation for various values of Hartmann number (M). It is seen from the figure that the effect of the Hartmann number is to decrease the fluid velocity. This is due to the production of Lorentz force which acts to oppose free flow of the fluid and hence act to retard the fluid flow. Further, the effect of Hartmann number on the micro-channels slip velocity becomes significant with increases in the wall-ambient temperature difference ratio (ξ).

Figure 4.2.4 shows the effect of suction/injection parameter (S) on the velocity. It is clear from this figure that as suction on the hot porous wall with simultaneous injection on the cold porous wall (that is $S > 0$) increases, the velocity decreases within the channel. This is attributed to the fact that cold fluid particles are injected into the micro-porous channel through the cold porous wall while fluid particles that are heated on the hot wall are removed out of the channel. This decreases the temperature in the channel thus weakening the convection current, which leads to a decrease in velocity. Furthermore, it is evident that the effect of suction/injection parameter (S) on the microchannel velocity slip and temperature jump becomes significant with decreases in the wall – ambient temperature difference ratio (ξ). The opposite phenomenon occurs when suction is applied on the cold porous wall with simultaneous injection on the hot porous wall ($S < 0$).

The variation of volume flow rate (Q) are displayed in Figure 4.2.5 with respect to fluid – wall interaction parameter (ln) and the departure from the continuum regime ($\beta_v Kn$) for various values of wall – ambient temperature difference ratio (ξ). From Figure 4.2.5, increasing $\beta_v Kn$ yields increases in volume flow rate (Q). It is interesting to note that as the

value of wall – ambient temperature difference ratio (ξ) increases, there are increases in the volume flow.

Figure 4.2.6 presents the variation of volume flow rate (Q) with respect to Hartmann number (M) and the departure from the continuum regime ($\beta_v Kn$) for various value of wall – ambient temperature difference ratios (ξ). We concluded from Figure 4.2.6 that as Hartmann number (M) increases, the volume flow rate decrease. This is due to the fact that, as the Hartmann number increases, the velocity decreases. It is also interesting to note that the role of Hartmann number is more significant for the case of symmetric heating ($\xi = 1$).

The variation of skin friction is revealed in Figures 4.2.7 and 4.2.8 with respect to fluid – wall interaction parameter (ln) and the departure from the continuum regime ($\beta_v Kn$) for various values of wall – ambient temperature difference ratios (ξ) at the microchannel plate $Y = 0$ and $Y = 1$, respectively. It is found from these figures that the skin-friction increases with the increases in the values of fluid – wall interaction parameter (ln). Also, it is observed that the impact of fluid-wall interaction parameter (ln) is insignificant for symmetric heating of micro-channel plates ($\xi = 1$).

Figures 4.2.9 and 4.2.10 shows the combined effects of Hartmann number (M) and the departure from the continuum regime ($\beta_v Kn$) for various values of wall – ambient temperature difference ratios (ξ) at the micro-channel plates $Y = 0$ and $Y = 1$, respectively. It is evident from the Figures that the skin-friction decreases with the increases in the values of Hartmann number (M) at $Y = 0$ while the reverse phenomenon occurs at $Y = 1$. In addition, the magnitude of skin-friction is higher in the case of symmetric heating ($\xi = 1$) in comparison to asymmetric heating of micro-channel plates ($\xi = 0$).

The variation of skin friction is presented in Figures 4.2.11 and 4.2.12 with respect to suction/injection parameter (S) and the departure from the continuum regime $(\beta_v Kn)$ for various values of wall – ambient temperature difference ratio (ξ) at the microchannel plate $Y = 0$ and $Y = 1$, respectively. It is seen from these figures that the skin - friction decreases with increases in rarefaction parameter $(\beta_v Kn)$ in the case of injection at $Y = 0$ and suction $Y = 1$ while the result is the reverse in the case of suction at $Y = 0$ and injection at $Y = 1$. It is seen that the particular cases of Equations (3.16) and (3.17) corresponding $M = 0$ reduces to the one in Equation (3.13). Furthermore, $S = 0$, Equation (3.17) agree with available results Equation (3.12).

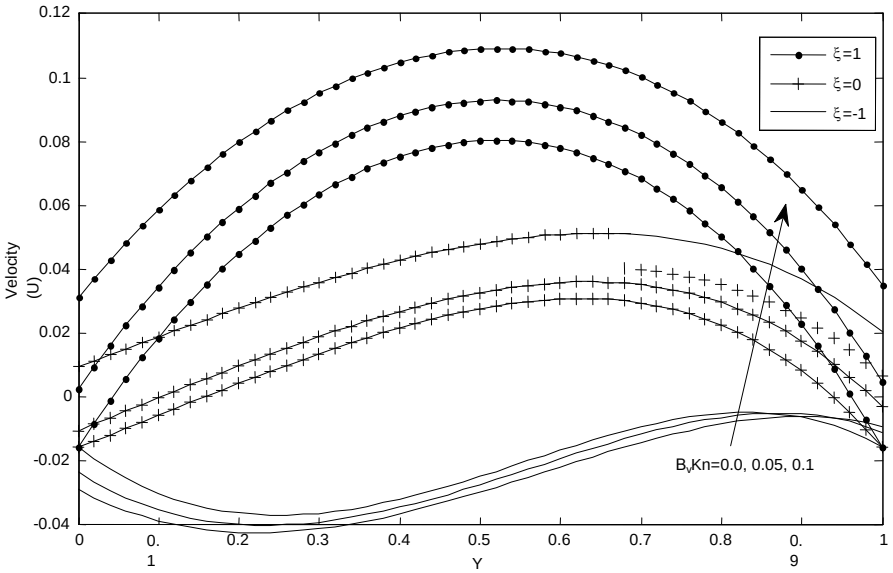


Figure 4.2.1: Velocity profile for various values of $\beta_v Kn$ (*ln = 1.667, S = 0.5, M = 2.0, Pr = 0.71*)

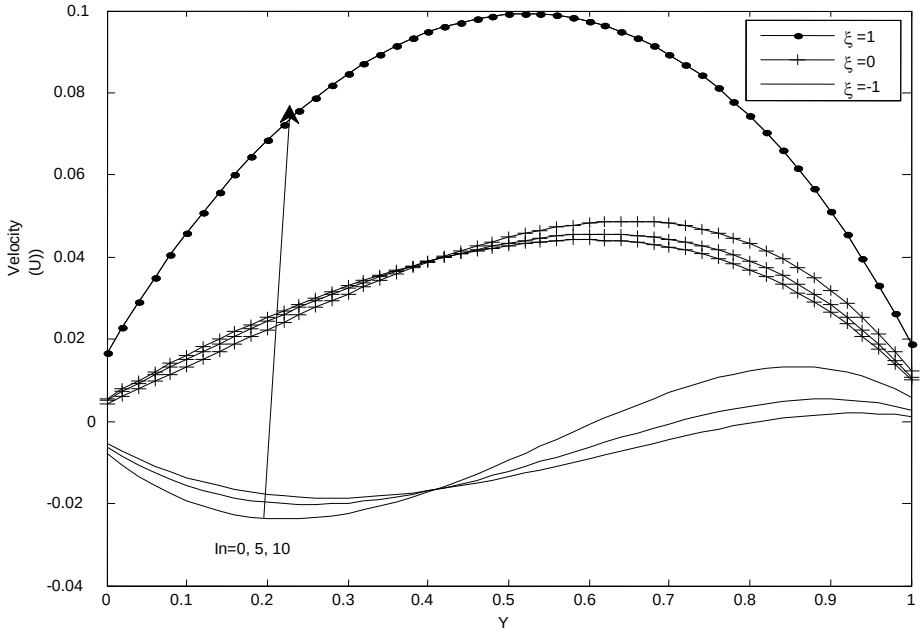


Figure 4.2.2: Velocity profile for various values of *ln* ($\beta_v Kn = 0.05$, *S = 0.5, M = 2.0, Pr = 0.71*)

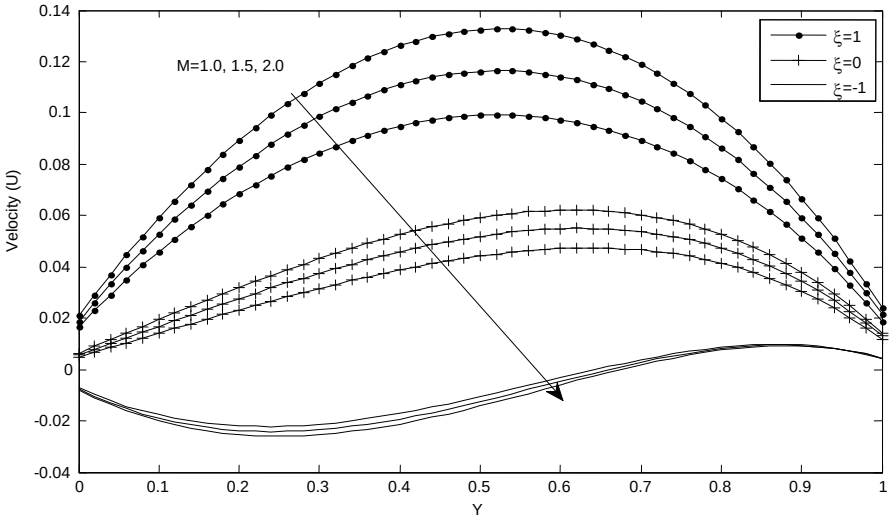


Figure 4.2.3: Velocity profile for various values of *M* ($\beta_v Kn = 0.05$, *S = 0.5, ln = 1.667, Pr = 0.71*)

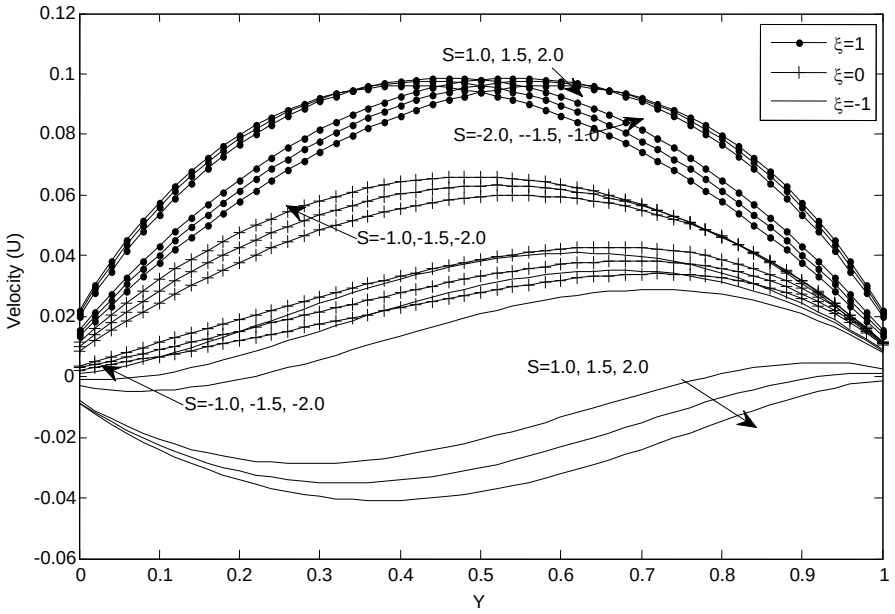


Figure 4.2.4: Velocity profile for various values of *S* ($\beta_v Kn$ = 0.05, *M* = 2.0, *ln* = 1.667, *Pr*=0.71)

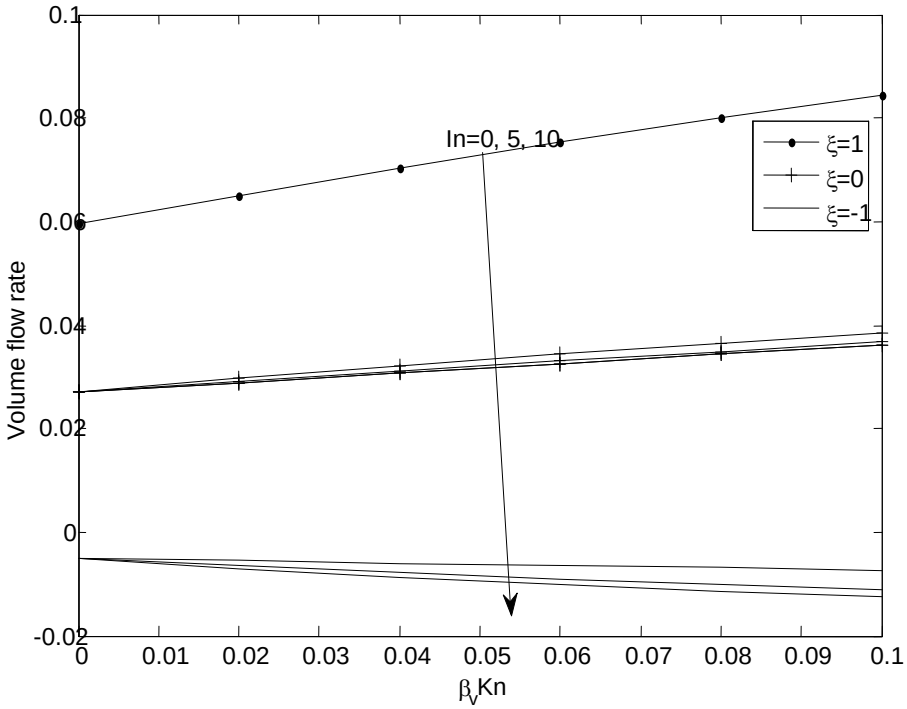


Figure 4.2.5: Relationship of Volume flow rate to *βvKn* for various values of *ln*

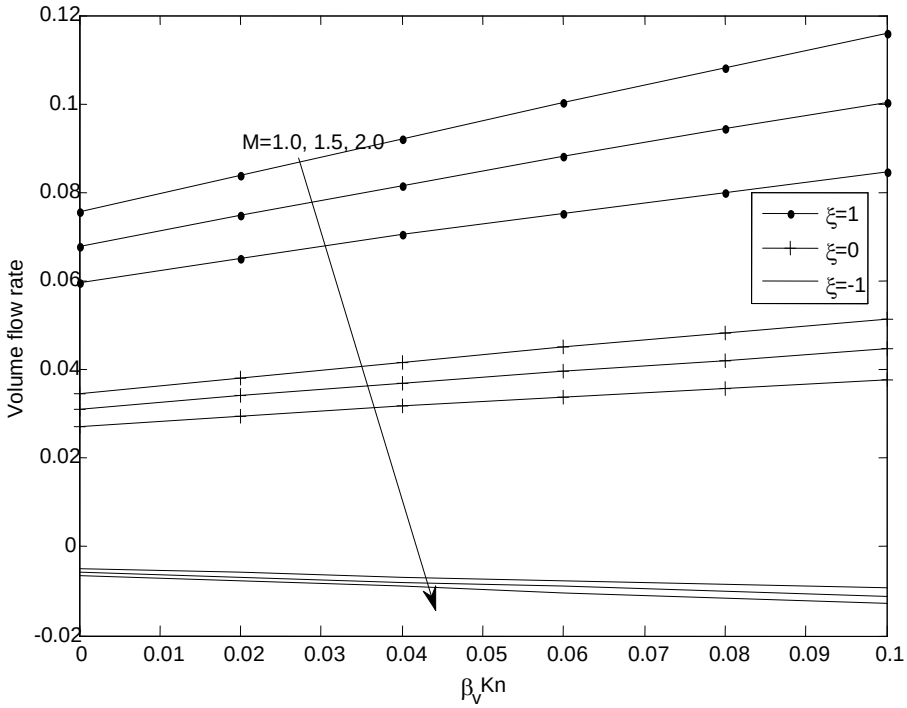


Figure 4.2.6: Relationship of Volume flow rate to $\beta_v Kn$ for various values of M

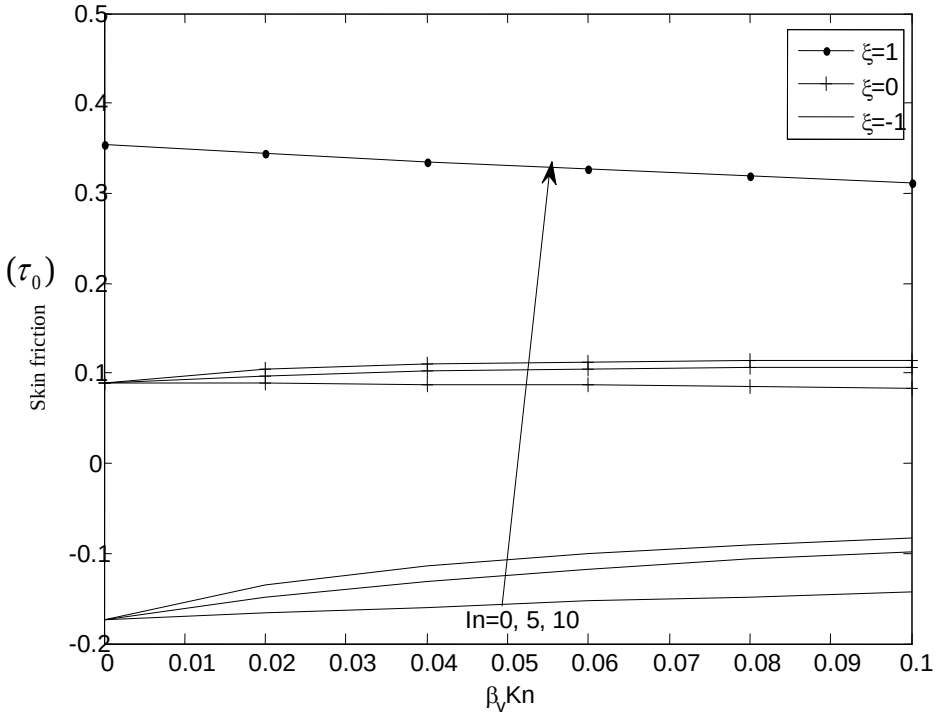


Figure 4.2.7: Variation of skin friction to various values of *ln* ($S = 0.5$, $M = 2.0$ ($Y = 0$))

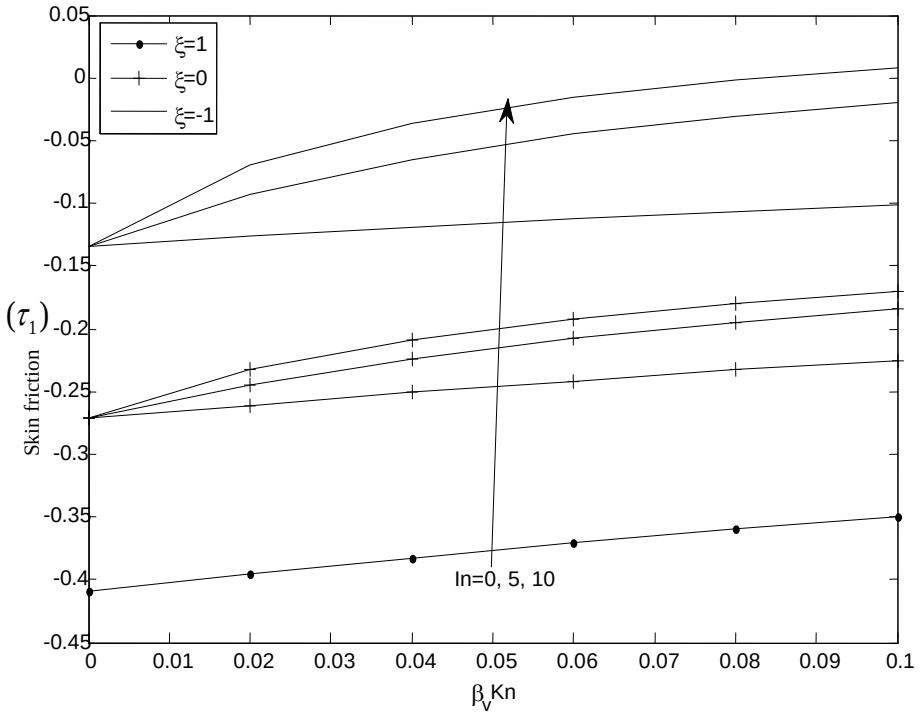


Figure 4.2.8: Variation of skin friction to various values of *ln* (*S = 0.5, M = 2.0* (*Y = 1*))

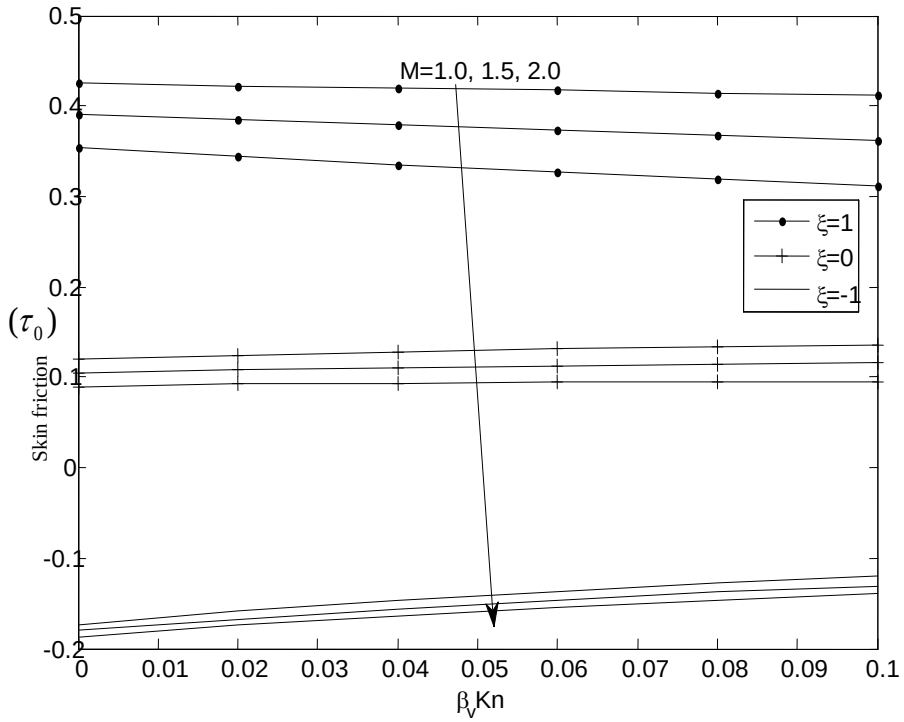


Figure 4.2.9: Variation of skin friction to various values of *M* (*S = 0.5, ln = 1.667* (*Y = 0*))

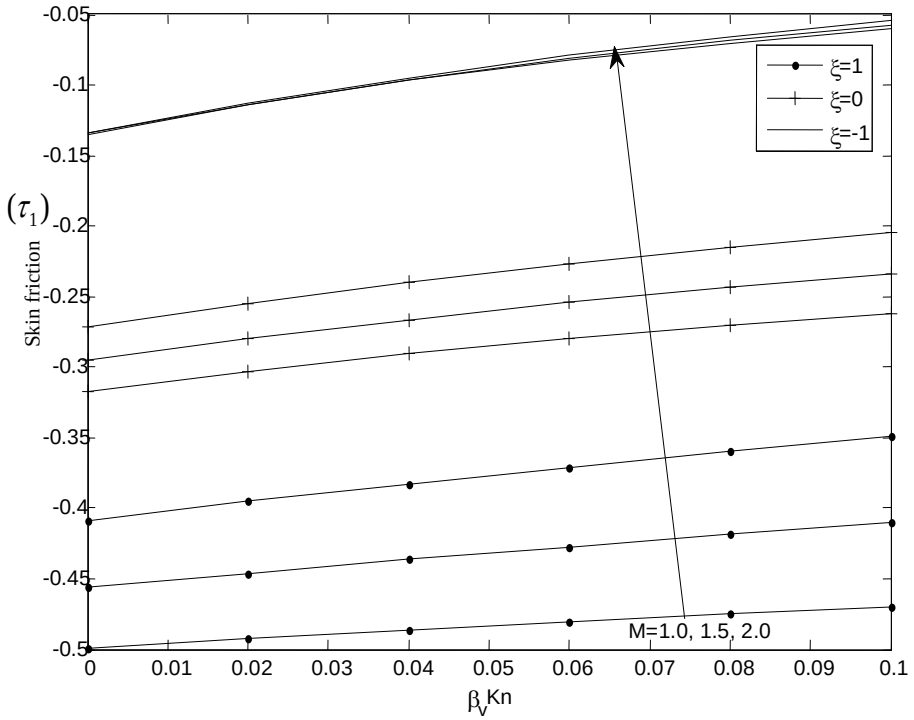


Figure 4.2.10 Variation of skin friction to various values of *M* (*S = 0.5, ln = 1.667* (*Y = 1*))

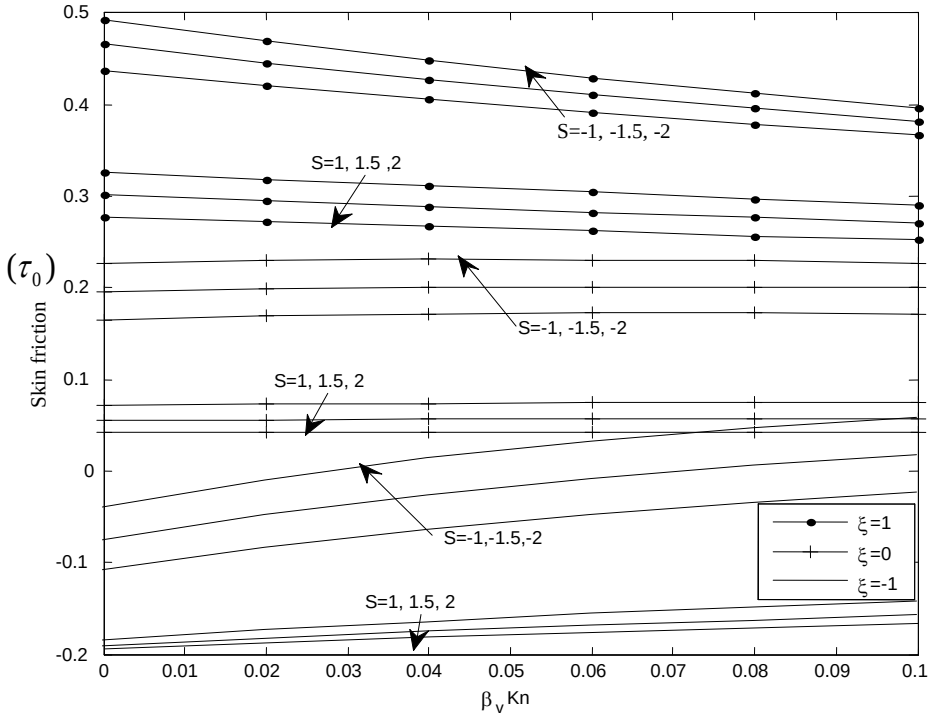


Figure 4.2.11: Variation of skin friction to various values of *S* (*M = 2.0, ln = 1.667* (*Y = 0*))

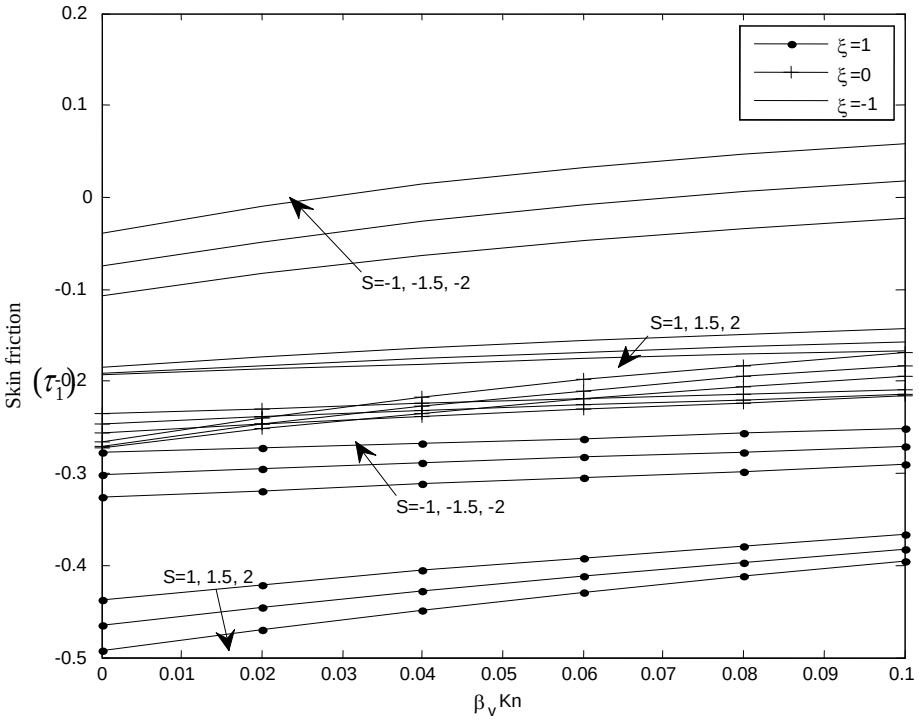


Figure 4.2.12: Variation of skin friction to various values of *S* (*M = 2.0, ln = 1.667* (*Y = 1*))

CHAPTER FIVE

SUMMARY, CONCLUSIONS AND RECOMMENDATIONS

5.0 Introduction

This chapter gives the summary, conclusions and recommendations of the whole work.

5.1 Summary

The first problem is the magnetohydrodynamic (MHD) natural convection flow in vertical parallel plates micro-channels. In this problem, the velocity slip and temperature jump at the plates are taken into consideration. The effect of various flow parameters entering into the problem such as Hartmann number, rarefaction parameter, and fluid-wall interaction parameter are discussed with the aid of line graphs. During the course of computation, it is found that increases in the effects of rarefaction and fluid wall interaction parameters leads to increases in the volume flow rate, while it decreases with increases of Hartmann number. In the second problem, exact solution of steady natural convection flow in vertical parallel plates micro-channels with combined effects of transverse magnetic field and suction/injection in the presence of velocity slip and temperature jump at the micro-channel surfaces. A closed-form solution is derived for velocity, temperature, volume flow rate, skin-friction and rate of heat transfer and is expressed as a Nusselt number. The effects of suction/injection parameter, Hartmann number, rarefaction parameter, and fluid-wall interaction parameter on the micro-channels hydrodynamic and thermal behaviours are analysed. Results show that as suction/injection, rarefaction and fluid-wall interaction increases, the volume flow rate increases, while it decreases with increases of Hartmann number. The implication of this is that the obtained results will help in the design of this type of engineering equipments that incorporates these basic fluid flow phenomena for the designed applications and in the aerodynamics field.

5.2 Conclusions

A theoretical study on steady magnetohydrodynamic fully developed natural convection flow in micro-channels has been presented. Closed-form expressions for velocity, temperature, volume flow rate, skin-friction and rate of heat transfer which is expressed as a Nusselt number are obtained by solving the present mathematical model. The effect of rarefaction parameter, fluid-wall interaction parameter, Hartmann number and suction/injection parameter are discussed with the aid of line graphs. The results showed that increases in the effects of rarefaction and fluid wall interaction leads to increases in the volume flow rate, while it decreases with increases in Hartmann number (M). It is also interesting to note that the role of Hartmann number on volume flow rate is insignificant for the case of symmetric heating ($\xi = 1$). In addition, it is observed that the skin-friction decreases with increases in the values of Hartmann number (M) at $Y = 0$, while the reverse phenomenon occurs at $Y = 1$. Furthermore, the magnitude of skin-friction is higher in the case of symmetric heating ($\xi = 1$) in comparison to asymmetric heating of micro-channel plates ($\xi = 0$).

It is also observed that the Hartmann number (M) becomes more significant as wall – ambient temperature difference ratio (ξ) increases. It is evident from this study that the effect of suction/injection parameter (S) on the microchannel velocity slip and temperature jump becomes significant with decreases in the wall – ambient temperature difference ratio (ξ). Also, it is observed that the skin-friction decreases with increases in the values of Hartmann number (M) at $Y = 0$, while the reverse phenomenon occurs at $Y = 1$. Finally, it is also observed that the skin - friction decreases with increases in rarefaction parameter ($\beta_v Kn$) in the case of injection at $Y = 0$ and suction $Y = 1$, while the result is the reverse in the case of suction at $Y = 0$ and injection at $Y = 1$. This study exactly agrees with the finding of Chen and Weng (2005) in the absence of transverse magnetic field and suction/injection parameter.

5.3 Recommendations

In this work, the steady natural convection flow of viscous, incompressible, electrically conducting fluid in vertical parallel plate micro-channels with combined effects of transverse magnetic field and suction/injection in the presence of velocity slip and temperature jump at the micro-channel surfaces as considered can be extended by taking into the unsteady natural convection flow of viscous, incompressible, electrically conducting fluid in vertical parallel plate micro-channels and is solved it by Laplace transform technique as well as numerical method and the obtained results compare with the exact solution discussed by other authors at large value of time.

This work provides an alternative solution to the problem Chen and Weng (2005). It is also an extension of the work of Chen and Weng (2005).

Therefore, it is recommended for use for the relevant applications in engineering or otherwise as the case may be.

REFERENCES

Al-jarrah J.A., Khadrawi A. F. and Al-Nimr M. A. (2008). Film condensation on a vertical micro- channel, *International Communication of Heat and Mass Transfer*. 35, 1173-1176.

Al-Sanea, (2004.)Mixed convection heat transfer along a continuously moving heated vertical plate with suction or injection. *International Journal of Heat Mass Transfer*. 47, 1445-1465.

Ashorynejad H. R., Sheikhholeslamia M., Pop I. and Gorji-Bandpy M., Ganji D. D. (2013). Nanofluid flow and heat transfer due a stretching cylinder in the presence magnetic field. *Int. Comm. Heat Mass Transfer*. 49:427-36.

Biswal L., Som S.K. and Chakraborry S. (2007). Effects of entrance region transport processes on free convection slip flow in vertical microchannels with isothermally heated walls, *International Journal of Heat Mass Transfer*. 50 (7-8) 1248-1254.

Chawla S. S. (1967). Magnetohydrodynamics unsteady free convection, *ZAMM*. 47, 499-508.

Chen C.K. and Weng H.C. (2005). Natural Convection in a Vertical Micro-channel, *Journal Heat Transfer*. 127**,** pp 1053-1056.

Cramer K. R. and Pai S. (2006). Magnetofluid dynamics for engineers and applied physicists. *Wiley Interscience*.

Haddad O.M., Abuzaid M.M. and Al-Nimr M.A. (A: 2005). Developing free-convection gas flow in a vertical open-ended microchannel filled with porous media, *Numer. Heat Transf*. 26(3), 905-918.

Ishak A., Merkin J. H., Nazar R. and Pop I. (1968). Mixed convection boundary layers flow over permeable vertical surface with prescribed plate heat flux. *Journal of Mathematical Physics*. 19:31-34.

Jha B. K., Aina B. and Joseph S. B. (2014). Natural Convection Flow in a Vertical Micro-Channel with Suction/Injection, *Journal of Process Mechanical Engineering.* 228(3), 171-180.

Khadrawi A.F, Othman A. and Al-Nimr M. A. (2005). Transient free convection gas flow in a Vertical Micro-channel as described by the hyperbolic heat conduction model, *International Journal Thermophysics*. 26(3): 905-918.

Larrode F. E., Housiadas C and Drossinos Y. (2000). Slip-flow heat transfer in circular tubes. *International Journal Heat and Mass Transfer*. 43:2669-80.

Rudraiah, N.; Barron, R. M., Venkatachalappa, M. & Subbaraya, C. K. (1995). Effect of a magnetic field on free convection in a rectangular enclosure. *International. Journal Engineering Science.* 33:1075-1084.

Seki, M.; Kawamura, H. & Sanokawa, K. (1979). Natural convection of mercury in a magnetic field parallel to the gravity. *Journal of Heat Transfer*. 101:227-232.

Sheikhholeslamia M., Gorji-Bandpy M. (2014).Free convection of ferrofluid in cavity heated from below in the presence of an external magnetic field. *Powder Technol*. 256:490-8.

Sheikhholeslamia M., Gorji-Bandpy M., and Ganji D. D. (2012). Magnetic field effects on natural convection around a horizontal circular cylinder inside a square enclosure filled with nanofluid. *Int. Comm. Heat Mass Transfer*. 39:978-86.

Sheikhholeslamia M., Gorji-Bandpy M., Ganji D. D. and Soleimani S. (2013). Effect of a magnetic field on natural convection in an inclined half-annulus enclosure filled with Cu-water nanofluid using CVFEM. *Powder Technol*. 24:980-91.

Sheikhholeslamia M., Gorji-Bandpy M., Ganji D. D. and Soleimani S. (2014). Natural convection heat and mass transfer in a cavity with sinusoidal wall filled with CuO-water nanofluid in the presence of magnetic fieldl. *Journal Taiwan Institute of chemical Engineering*. 45:40-90.

Sheikhholeslamia M., Gorji-Bandpy M., Ganji D. D., and Lattice B. (2014). Method for magnetohydrodynamic free convection heat transfer using nanofluid. *Powder Technol*. 245:82-93.

Sheikhholeslamia M., Gorji-Bandpy M., Ganji D. D., Ellahi R., Hassan M. and Soleimani S. (2014). Effects of magnetohydrodynamic on Cu-water nanofluid flow and heat transfer by means of CVFEM. *J. Magn Mater*. 349:188-200.

Sheikhholeslamia M., Gorji-Bandpy M., Ganji D. D., Rana P. and Soleimani S. (2014). Magnetohydrodynamic free convection of Al_2O_3-water nanofluid considering Thermophoresis and Brownian motion effects. *Compute Fluid*. 94:147-60.

Sheikhholeslamia M., Gorji-Bandpy M., Ganji D. D., Rana P. and Soleimani S. (2014). Magnetic field effects on nanofluid flow and heat transfer using KKL model. *Journal Taiwan Institute of chemical Engineering*. 45:795-807.

Sheikhholeslamia M., Gorji-Bandpy M., Ganji D. D., Rana P. Soleimani S. and Seyyedi S. M. (2012). Natural convection of nanofluid in an enclosure between a circular and a sinusoidal cylinder in the presence of magnetic field. *Int. Comm. Heat Mass Transfer*. 39:1435-43.

Singh A. K. (1984). Stokes problem for a porous vertical plate with sinks by finite difference method. *Astrophysics Space Science.* 103:241-248.

Soundalgekar V. M. and Takhar H. S. (1977). On MHD flow and heat transfer over a semi-infinite plate under transverse magnetic field, *Nucl. Eng. Des.* 42, 233-236.

Yu S. and Ameel T. A. (2001). Slip-flow heat transfer in a rectangular micro-channels. *International Journal Heat and Mass Transfer*. 44:4225-34.

APPENDIX I

List of constants used in defining temperature and velocity in problem 3.1

$$F_1 = \frac{A_0}{M^2}, \qquad F_2 = \frac{A_0}{M^2} + \frac{A_1}{M^2}, \qquad F_3 = \frac{A_1}{M^2}, \quad F_4 = 1 - \beta_v \mathrm{KnM}, \quad F_5 = \frac{\beta_v \mathrm{Kn} F_3 - F_1}{F_4},$$

$$F_6 = \exp(-M) - \frac{2\beta_v \mathrm{KnMexp}\ (\mathrm{M})}{F_4} - \frac{\exp(M)}{F_4} - \frac{(\beta_v \mathrm{Kn})^2 \mathrm{M}^2 \exp(M)}{F_4} - \beta_v \mathrm{KnMexp}(-\mathrm{M}),$$

$$F_7 = -\beta_v \mathrm{KnM} F_5 \exp(\mathrm{M}) - \beta_v \mathrm{Kn} F_3 - F_5 \exp(\mathrm{M}) - F_2$$

APPENDIX II

List of constants used in defining temperature and velocity in problem 3.2

$$F_1 = \beta_v KnInSPrexp(SPr) + \beta_v KnInSPr + exp(SPr) - 1$$

$$F_2 = \xi F_1 + \beta_v KnInSPr - \xi\beta_v KnInSPr + \xi - 1$$

$$F_3 = (SPr)^2 - S^2\Pr - M^2,\ F_4 = \frac{A}{M^2} - \frac{B}{F_3},\ F_5 = \frac{A}{M^2} - \frac{Bexp\,(SPr)}{F_3},\ F_6 = \frac{B(SPr)}{F_3}$$

$$F_7 = \frac{BSPr\ exp\,(SPr)}{F_3},F_8 = -\beta_v KnF_6 - F_4\ ,\ F_9 = 1 - \beta_v KnK_1$$

$$F_{10} = \frac{\beta_v KnK_2\exp(K_1)}{F_9} - \frac{\exp(K_1)}{F_9} + \exp(K_2) + \frac{(\beta_v Kn)^2 K_2 K_1\exp(K_1)}{F_9} - \frac{\beta_v KnK_1\exp(K_1)}{F_9} + \beta_v KnK_2\exp(K_1)$$

$$F_{11} = \beta_v KnF_7 - \frac{\beta_v Kn\,K_1\mathrm{F}_8\exp(K_1)}{F_9} - \frac{\mathrm{F}_8\exp(K_1)}{F_9} - F_5\ ,K_1 = \frac{S+\sqrt{S^2+4M^2}}{2},\ K_2 = \frac{S-\sqrt{S^2+4M^2}}{2}$$

APPENDIX III

Computer programs used to get the results of 3.1

VELOCITY DISTRIBUTION

```
clc;
y=1.0;
[y]=0.0:0.02:y;
m=1.0;
bvkn=0.0;
in=1.667;
g=1.0;
%g=0.0;
%g=-1;
a1=bvkn.*in.*(1-g);
a2=(1+2.*bvkn.*in);
a3=g;
a4=a1./a2;
A0=a3+a4;
a5=(1-g);
a6=(1+2.*bvkn.*in);
A1=a5./a6;
f1=(A0)./(m.^2);
f2=(A0)./(m.^2)+(A1)./(m.^2);
f3=(A1)./(m.^2);
f4=1-bvkn.*m;
f5=(bvkn.*f3-f1)./(f4);
f6=exp(-m)-(2.*bvkn.*m.*exp(m))./(f4)-(exp(m))./(f4)-((bvkn).^2.*m.^2.*exp(m))./(f4)-bvkn.*m.*exp(-m);
f7=-bvkn.*m.*f5.*exp(m)-bvkn.*f3-f5.*exp(m)-f2;
A=f5-(bvkn.*m.*f7)./(f4.*f6)-(f7)./(f4.*f6);
B=f7./f6;
Vel=A.*exp(m.*y)+B.*exp(-m.*y)+(A0)./(m.^2)+(A1.*y)./(m.^2);
hold on
```

```
Xlabel ({'Y'...
  ,'Figure 4,Velocity profile as a function M for \beta_vKn=0.05,In=1.667'})...
 ,Ylabel('Velocity (U)');
    plot(y,Vel,'.k','linestyle','-')
hold off
 clc;
 y=1.0;
 [y]=0.0:0.02:y;
  m=1.0;
  bvkn=0.0;
  in=1.667;
  g=1.0;
  %g=0.0;
  %g=-1;
a1=bvkn.*in.*(1-g);
a2=(1+2.*bvkn.*in);
a3=g;
a4=a1./a2;
A0=a3+a4;
a5=(1-g);
a6=(1+2.*bvkn.*in);
A1=a5./a6;
f1=(A0)./(m.^2);
f2=(A0)./(m.^2)+(A1)./(m.^2);
 f3=(A1)./(m.^2);
 f4=1-bvkn.*m;
 f5=(bvkn.*f3-f1)./(f4);
 f6=exp(-m)-(2.*bvkn.*m.*exp(m))./(f4)-(exp(m))./(f4)-((bvkn).^2.*m.^2.*exp(m))./(f4)-bvkn.*m.*exp(-m);
 f7=-bvkn.*m.*f5.*exp(m)-bvkn.*f3-f5.*exp(m)-f2;
 A=f5-(bvkn.*m.*f7)./(f4.*f6)-(f7)./(f4.*f6);
```

```
B=f7./f6;
Vel=A.*exp(m.*y)+B.*exp(-m.*y)+(A0)./(m.^2)+(A1.*y)./(m.^2);
hold on
Xlabel ({'Y'...
,'Figure 4,Velocity profile as a function M for \beta_vKn=0.05,In=1.667'})...
,Ylabel('Velocity (U)');
plot(y,Vel,'.k','linestyle','-')
hold off
% propertyeditor('on')
```

TEMPERATURE DISTRIBUTION

```
clc;
y=1.0;
[y]=0.0:0.02:y;
in=0;
bvkn=0.05;
%g=1.0;
%g=0.0;
g=-1;
a1=bvkn.*in.*(1-g);
a2=(1+2.*bvkn.*in);
a3=g;
a4=a1./a2;
A0=a3+a4;
a5=1-g;
a6=1+2.*bvkn.*in;
A1=a5./a6;
Tem=A0+A1.*y;
hold on
Xlabel ({'Y','Figure 3,Temperature profile as a function In for \beta_vKn=0.05 '})...
,Ylabel('Temperature');
```

```
    Plot(y,Tem,'k','linestyle',':')
  hold off
 % propertyeditor('on')
%natural convection in a vertical microchannel
 %Temperature distribution
 clc;
   y=1.0;
   [y]=0.0:0.02:y;
    in=0;
    bvkn=0.05;
    %g=1.0;
    %g=0.0;
    g=-1;
  a1=bvkn.*in.*(1-g);
  a2=(1+2.*bvkn.*in);
  a3=g;
  a4=a1./a2;
  A0=a3+a4;
  a5=1-g;
  a6=1+2.*bvkn.*in;
  A1=a5./a6;
  Tem=A0+A1.*y;
   hold on
  Xlabel ({'Y'...,'Figure 3,Temperature profile as a function In for \beta_vKn=0.05 '})...
   ,Ylabel('Temperature');
     plot(y,Tem,'k','linestyle',':')
  hold off
 % propertyeditor('on')
```

VOLUME FLOW RATE

```
   clc;
   bvkn=0.1;
```

```
 [bvkn]=0.0:0.02:bvkn;
  in=1.667;
  m=1.0;
  %g=1.0;
  %g=0.0;
  g=-1;
a1=bvkn.*in.*(1-g);
a2=(1+2.*bvkn.*in);
a3=g;
a4=a1./a2;
A0=a3+a4;
a5=(1-g);
a6=(1+2.*bvkn.*in);
A1=a5./a6;
f1=(A0)./(m.^2);
f2=(A0)./(m.^2)+(A1)./(m.^2);
 f3=(A1)./(m.^2);
 f4=1-bvkn.*m;
 f5=(bvkn.*f3-f1)./(f4);
 f6=exp(-m)-(2.*bvkn.*m.*exp(m))./(f4)-(exp(m))./(f4)-((bvkn).^2.*m.^2.*exp(m))./(f4)-bvkn.*m.*exp(-m);
 f7=-bvkn.*m.*f5.*exp(m)-bvkn.*f3-f5.*exp(m)-f2;
 A=f5-(bvkn.*m.*f7)./(f4.*f6)-(f7)./(f4.*f6);
 B=f7./f6;
 M=(A.*exp(m))./(m)-(B.*exp(-m))./(m)+(A0)./(m.^2)+(A1)./(m.^2)-(A)./(m)+(B)./(m);
 hold on
Xlabel ({'\beta_vKn'...,'Figure 6,Volume flow rate versus \beta_vKn different values of M'})...
 ,Ylabel('Volume flow rate');
plot(bvkn,M,'k','linestyle','-')
hold off
% propertyeditor('on')
```

SKIN FRICTION Y=0

```
clc;
bvkn=0.1;
[bvkn]=0.0:0.02:bvkn;
 m=1.0;
 in=1.667;
 %g=1.0;
 %g=0.0;
 g=-1;
a1=bvkn.*in.*(1-g);
a2=(1+2.*bvkn.*in);
a3=g;
a4=a1./a2;
A0=a3+a4;
a5=(1-g);
a6=(1+2.*bvkn.*in);
A1=a5./a6;
f1=(A0)./(m.^2);
f2=(A0)./(m.^2)+(A1)./(m.^2);
 f3=(A1)./(m.^2);
 f4=1-bvkn.*m;
 f5=(bvkn.*f3-f1)./(f4);
 f6=exp(-m)-(2.*bvkn.*m.*exp(m))./(f4)-(exp(m))./(f4)-((bvkn).^2.*m.^2.*exp(m))./(f4)-bvkn.*m.*exp(-m);
 f7=-bvkn.*m.*f5.*exp(m)-bvkn.*f3-f5.*exp(m)-f2;
 A=f5-(bvkn.*m.*f7)./(f4.*f6)-(f7)./(f4.*f6);
 B=f7./f6;
 Sk0=m.*A-m.*B+f3;
 hold on
Xlabel ({'\beta_vKn'...,'Figure 9,Variation of skin friction (\tau_0) for different values of M (Y=0)'})...
```

```
 ,Ylabel('skin friction (\tau_0)');
plot(bvkn,Sk0,'k','linestyle','-')
hold off
% propertyeditor('on')
```

SKIN FRICTION Y=1

```
clc;
bvkn=0.1;
[bvkn]=0.0:0.02:bvkn;
 m=1.0;
 in=1.667;
 %g=1.0;
 %g=0.0;
 g=-1;
a1=bvkn.*in.*(1-g);
a2=(1+2.*bvkn.*in);
a3=g;
a4=a1./a2;
A0=a3+a4;
a5=(1-g);
a6=(1+2.*bvkn.*in);
A1=a5./a6;
f1=(A0)./(m.^2);
f2=(A0)./(m.^2)+(A1)./(m.^2);
 f3=(A1)./(m.^2);
 f4=1-bvkn.*m;
 f5=(bvkn.*f3-f1)./(f4);
 f6=exp(-m)-(2.*bvkn.*m.*exp(m))./(f4)-(exp(m))./(f4)-((bvkn).^2.*m.^2.*exp(m))./(f4)-bvkn.*m.*exp(-m);
 f7=-bvkn.*m.*f5.*exp(m)-bvkn.*f3-f5.*exp(m)-f2;
 A=f5-(bvkn.*m.*f7)./(f4.*f6)-(f7)./(f4.*f6);
```

```
B=f7./f6;
Sk1=m.*A.*exp(m)-m.*B.*exp(-m)+f3;
 hold on
Xlabel ({'\beta_vKn'...,'Figure 10,Variation of skin friction(\tau_1) for different values of M (Y=1)'})...
,Ylabel('skin friction (\tau_1)');
plot(bvkn,Sk1,'k','linestyle','-')
hold off
% propertyeditor('on')
```

RATE OF HEAT TRANSFER

```
Nu=0
     clc;
     bvkn=0.1;
     [bvkn]=0.0:0.02:bvkn;
      in=0;
      %g=1.0;
      %g=0.0;
      g=-1;
    a1=bvkn.*in.*(1-g);
    a2=(1+2.*bvkn.*in);
    a3=g;
    a4=a1./a2;
    A0=a3+a4;
    a5=(1-g);
    a6=(1+2.*bvkn.*in);
    A1=a5./a6;
    de=A1;
      hold on
    Xlabel ({'\beta_vKn'...
      ,'Figure 9,Rate of heat transfer versus \beta_vKn for different
values of In '})...
```

```
      ,Ylabel('Nusselt nunmber (Nu)');
    plot(bvkn,de,'k','linestyle',':')
     hold off
    % propertyeditor('on')


Nu=1
    clc;
      bvkn=0.1;
      [bvkn]=0.0:0.02:bvkn;
       in=0;
       %g=1.0;
       %g=0.0;
       g=-1;
     a1=bvkn.*in.*(1-g);
     a2=(1+2.*bvkn.*in);
     a3=g;
     a4=a1./a2;
     A0=a3+a4;
     a5=(1-g);
     a6=(1+2.*bvkn.*in);
     A1=a5./a6;
     de=A1;
       hold on
     Xlabel ({'\beta_vKn'...
       ,'Figure 9,Rate of heat transfer versus \beta_vKn for different
values of In '})...
      ,Ylabel('Nusselt nunmber (Nu)');
     plot(bvkn,de,'k','linestyle',':')
     hold off
    % propertyeditorAppendix IV
```

Computer programs used to get the results of 3.2

VELOCITY DISTRIBUTION

```
clc;
y=1.0;
[y]=0.0:0.02:y;
pr=0.71;
in=1.667;
bvkn=0.05;
m=2.0;
s=-1.0;
%g=1.0;
%g=0.0;
g=-1;
f1=bvkn.*in.*s.*pr.*exp(s.*pr)+bvkn.*in.*s.*pr+exp(s.*pr)-1;
f2=g.*f1+bvkn.*in.*s.*pr-g.*bvkn.*in.*s.*pr-1+g;
A=f2./f1;
B=(1-g)./(f1);
f3=(s.*pr).^2-s.^2.*pr-m.^2;
f4=(A)./(m.^2)-(B)./(f3);
f5=(A)./(m.^2)-(B.*exp(s.*pr))./(f3);
f6=(B.*s.*pr)./(f3);
f7=(B.*s.*pr.*exp(s.*pr))./(f3);
f8=-bvkn.*f6-f4;
    k1=(s+sqrt(s.^2+4.*m.^2))./(2);
k2=(s-sqrt(s.^2+4.*m.^2))./(2);
f9=1-bvkn.*k1;
f10=(bvkn.*k2.*exp(k1))./(f9)-(exp(k1))./(f9)+exp(k2)+((bvkn).^2.*k2.*k1.*exp(k1))./(f9)-
(bvkn.*k1.*exp(k1))./(f9)+(bvkn.*k2.*exp(k2));
f11=bvkn.*f7-(bvkn.*k1.*exp(k1).*f8)./(f9)-(f8.*exp(k1))./(f9)-f5;
```

```
Cc=(bvkn.*k2.*f11)./(f9.*f10)-(f11)./(f9.*f10)+(f8)./(f9);
D=(f11)./(f10);
Vel=Cc.*exp(k1.*y)+D.*exp(k2.*y)+(A)./(m.^2)-(B.*exp(s.*pr.*y))./(f3);
   hold on
Xlabel ({'Y'...,'Figure 5,Velocity profile as a function S for \beta_vKn=0.05,M=2.0,In=1.667,Pr=0.71'})...
 ,Ylabel('Velocity (U)');
   plot(y,Vel,'k','linestyle','-')
hold off
% propertyeditor('on')
```

VOLUME FLOW RATE

```
  clc;
 bvkn=0.1;
 [bvkn]=0.0:0.02:bvkn;
  pr=0.71;
  in=1.667;
  m=1.0;
  s=0.5;
  %g=1.0;
  g=0.0;
  %g=-1;
f1=bvkn.*in.*s.*pr.*exp(s.*pr)+bvkn.*in.*s.*pr+exp(s.*pr)-1;
f2=g.*f1+bvkn.*in.*s.*pr-g.*bvkn.*in.*s.*pr-1+g;
A=f2./f1;
B=(1-g)./(f1);
f3=(s.*pr).^2-s.^2.*pr-m.^2;
f4=(A)./(m.^2)-(B)./(f3);
f5=(A)./(m.^2)-(B.*exp(s.*pr))./(f3);
f6=(B.*s.*pr)./(f3);
f7=(B.*s.*pr.*exp(s.*pr))./(f3);
```

```
f8=-bvkn.*f6-f4;
k1=(s+sqrt(s.^2+4.*m.^2))./(2);
k2=(s-sqrt(s.^2+4.*m.^2))./(2);
f9=1-bvkn.*k1;
f10=(bvkn.*k2.*exp(k1))./(f9)-(exp(k1))./(f9)+exp(k2)+((bvkn).^2.*k2.*k1.*exp(k1))./(f9)-
(bvkn.*k1.*exp(k1))./(f9)+(bvkn.*k2.*exp(k2));
f11=bvkn.*f7-(bvkn.*k1.*exp(k1).*f8)./(f9)-(f8.*exp(k1))./(f9)-f5;
  Cc=(bvkn.*k2.*f11)./(f9.*f10)-(f11)./(f9.*f10)+(f8)./(f9);
D=(f11)./(f10);
M=(Cc.*exp(k1))./(k1)+(D.*exp(k2))./(k2)+(A)./(m.^2)-(B.*exp(s.*pr))./(f3.*s.*pr)-(Cc)./(k1)-
(D)./(k2)+(B)./(f3.*s.*pr);
 hold on
Xlabel ({'\beta_vKn'... ,'Figure 7,Volume flow rate versus \beta_vKn for dif
```

SKIN FRICTION Y=0

```
clc;
 bvkn=0.1;
 [bvkn]=0.0:0.02:bvkn;
  pr=0.71;
  in=0;
  m=2.0;
  s=0.5;
  %g=1.0;
  %g=0.0;
  g=-1;
f1=bvkn.*in.*s.*pr.*exp(s.*pr)+bvkn.*in.*s.*pr+exp(s.*pr)-1;
f2=g.*f1+bvkn.*in.*s.*pr-g.*bvkn.*in.*s.*pr-1+g;
A=f2./f1;
B=(1-g)./(f1);
f3=(s.*pr).^2-s.^2.*pr-m.^2;
```

```
    f4=(A)./(m.^2)-(B)./(f3);
    f5=(A)./(m.^2)-(B.*exp(s.*pr))./(f3);
    f6=(B.*s.*pr)./(f3);
    f7=(B.*s.*pr.*exp(s.*pr))./(f3);
    f8=-bvkn.*f6-f4;
     k1=(s+sqrt(s.^2+4.*m.^2))./(2);
    k2=(s-sqrt(s.^2+4.*m.^2))./(2);
    f9=1-bvkn.*k1;
    f10=(bvkn.*k2.*exp(k1))./(f9)-(exp(k1))./(f9)+exp(k2)+((bvkn).^2.*k2.*k1.*exp(k1))./(f9)-
(bvkn.*k1.*exp(k1))./(f9)+(bvkn.*k2.*exp(k2));
    f11=bvkn.*f7-(bvkn.*k1.*exp(k1).*f8)./(f9)-(f8.*exp(k1))./(f9)-f5;
    Cc=(bvkn.*k2.*f11)./(f9.*f10)-(f11)./(f9.*f10)+(f8)./(f9);
    D=(f11)./(f10);
   Sk0=Cc.*k1+D.*k2-f6;
  hold on
    Xlabel ({'\beta_vKn'...,'Figure 12,Variation of skin friction for different values of S for
M=2,In=1.667(Y=0)'})...
     ,Ylabel('Skin friction (\tau_0)');
      plot(bvkn,Sk0,'k','linestyle',':')
    hold off
   % propertyeditor('on')
ferent values of M'})...
     ,Ylabel('Volume flow rate');
    plot(bvkn,M,'k','linestyle','-.')
    hold off
   % propertyeditor('on')


SKIN FRICTION Y=1

    clc;
```

```
bvkn=0.1;
[bvkn]=0.0:0.02:bvkn;
pr=0.71;
in=0;
m=2.0;
s=0.5;
%g=1.0;
%g=0.0;
g=-1;
f1=bvkn.*in.*s.*pr.*exp(s.*pr)+bvkn.*in.*s.*pr+exp(s.*pr)-1;
f2=g.*f1+bvkn.*in.*s.*pr-g.*bvkn.*in.*s.*pr-1+g;
A=f2./f1;
B=(1-g)./(f1);
f3=(s.*pr).^2-s.^2.*pr-m.^2;
f4=(A)./(m.^2)-(B)./(f3);
f5=(A)./(m.^2)-(B.*exp(s.*pr))./(f3);
f6=(B.*s.*pr)./(f3);
f7=(B.*s.*pr.*exp(s.*pr))./(f3);
f8=-bvkn.*f6-f4;
k1=(s+sqrt(s.^2+4.*m.^2))./(2);
k2=(s-sqrt(s.^2+4.*m.^2))./(2);
f9=1-bvkn.*k1;
f10=(bvkn.*k2.*exp(k1))./(f9)-(exp(k1))./(f9)+exp(k2)+((bvkn).^2.*k2.*k1.*exp(k1))./(f9)-
(bvkn.*k1.*exp(k1))./(f9)+(bvkn.*k2.*exp(k2));
f11=bvkn.*f7-(bvkn.*k1.*exp(k1).*f8)./(f9)-(f8.*exp(k1))./(f9)-f5;
Cc=(bvkn.*k2.*f11)./(f9.*f10)-(f11)./(f9.*f10)+(f8)./(f9);
D=(f11)./(f10);
Sk0=Cc.*k1+D.*k2-f6;
hold on
```

```
    Xlabel ({'\beta_vKn'...,'Figure 12,Variation of skin friction for different values of S for
M=2,In=1.667(Y=0)'})...
     ,Ylabel('Skin friction (\tau_0)');
    plot(bvkn,Sk0,'k','linestyle',':')
    hold off
   % propertyeditor('on')
ferent values of M'})...
     ,Ylabel('Volume flow rate');
    plot(bvkn,M,'k','linestyle','-.')
    hold off
   % propertyeditor('on')
```

NUSSELT NUMBER NU=0

```
    clc;
     bvkn=0.1;
     [bvkn]=0.0:0.02:bvkn;
     pr=0.71;
      in=0;
      s=0.5;
      %g=1.0;
      %g=0.0;
      g=-1;
    f1=bvkn.*in.*s.*pr.*exp(s.*pr)+bvkn.*in.*s.*pr+exp(s.*pr)-1;
    f2=g.*f1+bvkn.*in.*s.*pr-g.*bvkn.*in.*s.*pr-1+g;
    A=f2./f1;
    B=(1-g)./(f1);
    Nu0=B.*s.*pr;
     hold on
    Xlabel ({'\beta_vKn'...,'Figure 11,Rate of heat transfer versus \beta_vKn for different values of In (Y=0)'})...
     ,Ylabel('Nusselt number');
    plot(bvkn,Nu0,'k','linestyle',':')
```

```
 hold off
% propertyeditor('on')
```

NUSSELT NUMBER NU=1

```
clc;
 bvkn=0.1;
 [bvkn]=0.0:0.02:bvkn;
  pr=0.71;
  in=0;
  s=0.5;
  %g=1.0;
  %g=0.0;
  g=-1;
f1=bvkn.*in.*s.*pr.*exp(s.*pr)+bvkn.*in.*s.*pr+exp(s.*pr)-1;
f2=g.*f1+bvkn.*in.*s.*pr-g.*bvkn.*in.*s.*pr-1+g;
A=f2./f1;
B=(1-g)./(f1);
Nu1=B.*s.*pr.*exp(s.*pr);
 hold on
Xlabel ({'\beta_vKn'...,'Figure 12,Rate of heat transfer versus \beta_vKn for different values of In (Y=1)'})...
 ,Ylabel('Nusselt number');
plot(bvkn,Nu1,'k','linestyle',':')
hold off
% propertyeditor('on')
```